DESIGN AND EVALUATION OF AN OFFLOADING ORTHOSIS FOR MEDIAL KNEE OSTEOARTHRITIS

MADELEINE ALORA-IVY IMBODEN

Thesis submitted to the University of Ottawa
in partial Fulfillment of the requirements for the
Master of Applied Science Mechanical Engineering

Ottawa-Carleton Institute for Mechanical and Aerospace Engineering
Department of Mechanical Engineering
Faculty of Engineering
University of Ottawa

Abstract

Knee osteoarthritis is an incurable degenerative joint disease that affects millions of people in Canada. Characterized by stiffness and knee pain in the early stages, it can cause loss of function and mobility. Most treatment options are either not sustainable, such as pain medications and steroid injections, or invasive, such as knee replacement surgery. While therapeutic options, such as physiotherapy, have been shown to have a positive effect on pain and activity levels over time, minimal immediate relief has been observed. Moreover, these treatments or combinations of treatments can be costly.

Alternatively, offloading knee orthoses are a cost-effective option that provides immediate pain relief when worn. Offloading knee orthoses, however, have low patient compliance rates. To improve patient compliance and optimize patient benefit, current orthosis designs must be enhanced to improve comfort, increase the perceived effect and be adjustable to the patient.

Consequently, this thesis presents the design, fabrication and testing of an offloading knee orthosis joint designed to enhance comfort and perceived effect. This improvement is achieved by developing a novel modular orthosis that features an offloading mechanism intended to relieve the load on the joint through an offloading moment solely during stance phase and reduce the moment during swing phase when offloading is not needed. The evaluation of the proposed orthosis design was achieved by fabricating an experimental prototype and performing mechanical testing. Three-point bending tests demonstrated a generated offloading moment of 3.36 Nm, creating a noticeable offloading effect during stance, and reduced the moment to less than 0.5 Nm after 35° of knee flexion, thus, increasing comfort during swing phase and sitting when offloading forces are not needed.

Acknowledgements

I would like to thank my supervisor, Dr. Doumit, for his guidance and support throughout this project.

I would also like to thank the University of Ottawa Manufacturing Center, especially Paul Burberry, who helped troubleshoot SolidWorks backwards compatibility, suggested manufacturing options and brought the prototype to life.

Last but not least, I would like to thank my family. My parents, for supporting me throughout my school career. My dad for always listening to my prototype ideas and finding the silver lining in my failures. My fiancé, Zack Levi, for proofreading this paper, supplying coffee, and encouraging me throughout my school years.

Table of Contents

List of Figures

List of Tables

Chapter 1- Introduction

Osteoarthritis (OA) is an increasingly prevalent joint disease that affects over 10% of the Canadian population over the age of 15 [1]. In Canada, it is estimated that 6 million people will be affected by OA by 2031, a significant increase from the OA population in 2010 of 2.6 million [2]. OA is characterized by knee stiffness, pain and loss of physical function, typically resulting from pathophysiological and structural changes within the joint [3], [4].

Current interventions are centred around reducing pain, improving physical function and health-related quality of life as there is no cure for OA [5]. Pharmacological approaches can treat pain and inflammation; there are also ongoing studies on drugs to stop further degradation of the OA-affected joint [6]–[8]. However, pharmacological interventions are often not recommended for long-term use, and their long-term effectiveness is uncertain [8]–[10]. Studies estimate that societal costs related to opioids, specifically in knee OA treatment, including addiction and lost workplace productivity, nearly match the direct medical costs, making it a costly treatment option [11]. In advanced OA cases, where there is severe cartilage loss causing bone on bone contact, joint replacements or other surgical interventions are performed [5]. Nearly 99% of knee replacement patients reported to the Canadian Joint Replacement Registry in the 2017-2018 annual report had an OA diagnosis [12]. Primary knee replacements are estimated to cost about $7800, whereas revision surgeries, often more risky and complicated, cost nearly double and amounted to over $74 million in revision inpatient costs [12]. Risk factors for revision surgery include young patient age, male sex, and pre-operative joint stiffness [12]–[14].

In Ontario, according to published targets, it takes 182 days to see a surgeon after referral and an additional 182 days between the decision and surgery. However, actual waiting times vary significantly in Ontario. For example, Perth and Smith Falls District hospital reported an average wait time of 289 days. Other provinces in Canada are not fairing any better, with significant increases in wait times [15]. A 2019 report showed that wait times for knee replacement surgery increased 41% in PEI between 2016 and 2018 and 21% in Manitoba during the same time frame [15]. With the ageing Canadian population, increased OA patient population, and the high costs of surgical intervention, alternative treatment options for OA must be explored.

Therapeutic treatment of OA, including knee braces, has been recommended by the Osteoarthritis Research Society, European League Against Rheumatism, and the National Institute for Clinical Excellence [16], [17]. While there are many varieties of knee braces, including rest braces and knee sleeves, studies performed on offloading knee braces have consistently shown positive results in unicompartmental OA with a reduction in pain, increased activity and potential to delay surgical intervention [16]–[18]. Offloading orthoses apply a counter moment to the knee to help unload the affected compartment. The offloading moment increases joint space in the compartment, which in turn reduces pain.

Unfortunately, while offloading orthoses present a variety of short-term and long-term benefits to patients, compliance in wearing braces is meagre and is reported to be as low as 28% after the first fitting [19]. A major complaint from patients is lack of comfort and lack of perceived effect while wearing the brace [19]. However, a recent study demonstrated that wearing an offloading orthosis can have benefits even in the short term. An eight-year study completed in the U.K. showed that wearing an offloading knee orthosis for at least six months halved the patient's need to have surgery compared to those who wore an offloading brace for three months or less [18]. Furthermore, all patients in the study who wore the brace for at least 24 months opted out of surgical intervention (confirmed at an eight-year follow-up) [18]. The study demonstrated offloading braces as a cost-effective bridging treatment to surgery and a possible method to delay or reduce the need for surgical intervention. Multiple other studies have shown benefits in lowering revision surgery risks such as increased activity, muscle strengthening and increased stability [20].

While great success has been achieved with current offloading designs, additional benefits can be attained with orthosis design optimization. This thesis proposes an offloading knee brace joint that applies variable offloading forces to increase patient comfort and the perceived effect of the brace. Increasing comfort and perceived effect may encourage the patient to wear the offloading brace for a more effective period, improve patient quality of life, decrease or delay surgical intervention, and decrease the financial burden on the health care system.

1.1 Objectives

The goal of this thesis is to develop and test a novel variable offloading knee orthosis joint to improve patient comfort and perceived effect. The orthosis joint design must incorporate an offloading mechanism to achieve variable joint loading during stance phase and reduce the offloading moment during swing phase.

1.2 Methodology

First, to achieve the research objectives, the mechanical deflection required to produce the joint offloading moment was characterized through a mechanical model. Next, using Computer-Aided Design, a prototype was developed to achieve the distinct attributes of the variable offloading orthosis joint. Subsequently, the prototype was fabricated in the laboratory and mechanically tested to demonstrate its performance. Finally, the experimental results were compared to the mechanical model to validate the initial hypothesis and verify that variable offloading can be achieved through the proposed design.

1.3 Contributions

This thesis contains a comprehensive literature review on the current state of offloading orthoses and potential analysis regarding developing a variable offloading knee joint to reduce symptoms related to patient acceptance and perceived effect.

This thesis presents a novel and modular design approach to achieve variable knee offloading. Variable offloading differs from current popular designs that apply a constant magnitude of offloading throughout the knee's range of motion (ROM). The proposed design uses offloading when it is most effective, and its modular design allows for easy adjustment to fit the user’s activity and comfort. Moreover, the proposed design demonstrates offloading potential in low degrees of flexion.

1.4 Thesis Outline

This thesis contains six chapters. Chapter 1 serves as an introduction to OA and dynamic offloading orthoses as a proposed solution to the limitations of current interventions. The objective, methods and contributions of the thesis are also contained within this chapter.

Chapter 2 reviews current literature, including osteoarthritic pathologies, gait dynamics and current offloading devices.

Chapter 3 introduces the design of the proposed variable offloading joint. This chapter includes the design criteria, the SolidWorks drawings and the manufactured prototype.

Chapter 4, a mechanical bending model is derived, and simulation of the model presented. Differences between the model and observed values are compared and discussed.

Chapter 5 outlines the experimental method followed during the three-point bending mechanical test. It also presents and examines the results of the experimental testing.

Chapter 6 concludes this dissertation and presents areas for future work.

Chapter 2- Literature Survey

This section addresses the current literature, starting with a brief overview of OA and related gait pathologies. An overview of existing interventions follows, concluding with a presentation of the efficacy and challenges of current interventions.

This review concentrates on OA affecting the medial tibial femoral knee compartment as it is 5-10 times more prevalent than lateral OA in Western populations [21], [22].

2.1 Overview of Knee Osteoarthritis

OA is a prevalent degenerative joint disease that causes progressive destruction of knee structures such as cartilage, subchondral bone surfaces, and the synovial membrane. It is characterized by knee stiffness, pain, and loss of physical function, which are typically a result of the pathophysiological and structural changes within the joint [3], [4]. Studies in the U.S. demonstrate that obesity, age and female gender can increase the lifetime risk of knee OA diagnosis [23]. Approximately 9% of the U.S. population is diagnosed with this disease by age 60, with the median diagnosis age of 55 [23].

Knee OA is typically confirmed through radiographic evidence and can be categorized by severity into a grading system, like Kellgren Lawrence, based on joint space, osteophytes, sclerosis, and bone contour. Figure 1 demonstrates radiographic OA features of Kellgren Lawrence grades 1 through 4.

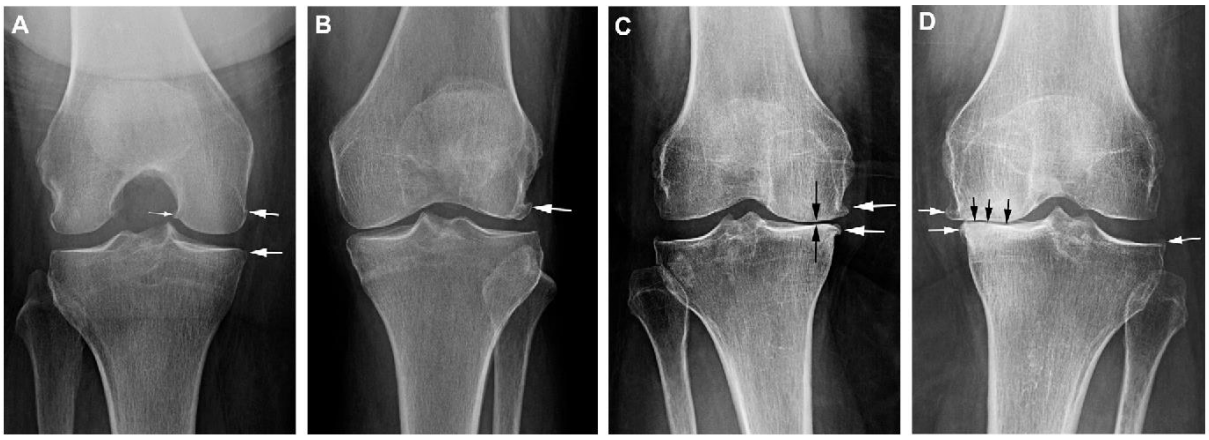

Figure 1: Radiographic images of Kellgren- Lawrence grades 1-4. (A) grade 1, minimal formation of osteophytes at arrows. (B) grade 2, evident osteophyte. (C) grade 3, joint space narrowing, in addition to osteophytes. Image (D), grade 4, bone to bone contact and osteophytes [24].

There are two main types of knee OA; the first and most common is the degeneration of the joint cartilage over time with regular use. Secondary OA is typically caused by trauma, obesity, or other

diseases such as rheumatoid arthritis. However, both primary and secondary OA follow the same treatment plans.

The main treatment goals are pain reduction and increasing or maintaining function, mobility, and health-related quality of life [25]. There are various treatments available, from physical therapy, gait retraining, orthoses, intra-articular injections, and pain medications to more invasive options such as high tibial osteotomies, partial and total knee replacements.

2.2 Gait Pathologies

Gait changes in individuals with OA vary with the severity and the progression of the disease. However, most patients with mild to severe cases often alter their gait to unload the compartment affected by OA, but gait changes may be induced by other symptoms [26]. Studies show that pain and knee instability may also impact the gait of patients. For example, a study compared gait changes in healthy subjects when exposed to knee pain induced by saline injections [27]. The results showed that when healthy subjects had knee pain, their gait changes closely resembled less severe OA patients [27]. This suggests that gait changes may be induced by pain in less severe cases and not just attempts at offloading damaged knee compartments [27].

Additionally, there is a tendency for individuals with OA to alter their gait to reduce the knee adduction moment. The knee adduction moment is often associated with medial loading and knee pain, with the magnitude of the moment and related symptoms increasing as the disease progresses [28]–[30]. The adduction moment of the knee has become a widely studied gait parameter and is often used to measure both disease progression and severity [28]. Some therapeutic treatment options aim to reduce pain by reducing the knee adduction moment. They will be presented in the next section.

Knee flexion is another crucial parameter. However, its moment is less meaningful when estimating disease severity and progression as the knee flexion moment is often similar between subjects with moderate and severe OA [28] [31]. Both the ROM and moment of knee flexion are reduced in subjects with OA when compared with healthy controls [31]. In a study of 23 individuals with OA with matched controls, knee flexion during stance was reduced by nearly 8°, while flexion during swing decreased by an average of 6.4° [31]. It has also been demonstrated

that the knee flexion angle is increased at heel strike, indicating a lack of extension during gait in individuals with OA [28], [30], [32].

People affected with OA tend to lose muscle strength as the disease progresses and can be a factor leading to OA and its progression [33]–[35]. Quadriceps muscle strength reduction varies from 15-18% before disease diagnosis, increasing to 24% loss with patients diagnosed with Kellgren Lawrence grade II OA and 38% with grade IV [34], [35]. Many studies have linked quadriceps deficit to OA progression. Theories of muscle weakness include reduced voluntary muscle activation, joint pain and instability leading to reduced activity, increased age-related muscle loss and muscle dysfunction [33]–[37]. Quadriceps muscle weakness in women with OA causes gait irregularities such as shortened swing phase, longer support time and reduced speed [38]. It is important to note that antagonist co-contraction has not been associated with flexion and quadriceps extension weakness [39].

While quadriceps strength tends to be heavily researched, hamstring strength is also an essential component of maintaining proper muscle balance at the knee [40]–[42]. Hamstring deficits for individuals with OA range from 4-35% in isometric tests and 7-38% in isokinetic tests [40]. In healthy individuals, the mean isometric quadriceps strength to hamstring strength ratio is approximately 2:1. However, with knee OA, this ratio is reduced to 1.43:1 [42]. As hamstring strength is vital to many basic movements such as stair climbing, sit-to-stand and walking, it is evident why hamstring strength has been negatively correlated with higher self-perceived functional limitations by individuals with OA [40], [43]. It is important to strengthen and maintain the balance between the hamstring and quadriceps during rehabilitation to avoid interference of normal load and muscle distribution at the knee [41], [44].

Impaired proprioception in individuals with OA is linked with disease progression, knee pain and activity limitations [45] [46]. Resistance training has been shown to reduce pain and functional declines and improve proprioception [46], [47]. Strengthening muscles in subjects also has another benefit as pre-operative functional status and strength may enhance postoperative recovery and be used as an indicator of the physical function of the knee one year after knee replacement [44], [48], [49].

2.3 Offloading Orthoses

As medial compartment tibial femoral osteoarthritis is most common, this section concentrates on valgus-producing braces [21], [22]. A valgus offloading brace realigns the knee joint towards the lateral compartment and can be used therapeutically for subjects with mild to severe medial OA [50]. The external valgus force applied by the brace to the knee joint realigns the tibiofemoral interface. This unloads the affected medial compartment and increases joint space in that area [50]–[53].

Both custom and off-the-shelf bracing options are available for unicompartmental offloading; however, studies have demonstrated that custom-fit braces have more benefits in terms of pain reduction, better alignment and comfort [17], [54], [55].

In this section, the effects of offloading knee orthosis use, including pain reduction, increased knee function, and long-term benefits, will be presented.

2.3.1.1 Knee Pain and Function

Pain is one of the main complaints made by individuals with OA, and it is also one of the leading causes of disability and loss of independence in senior patients [56]. Pain reduction is a primary goal of OA management to improve patient quality of life [57]. Reducing pain also has the benefit of decreasing the amount of pain medication a patient takes, which can reduce costs and be beneficial to overall patient health [58]. Thus, pain is an essential measure in the effectiveness and probable compliance in subjects wearing braces. Pain scales such as the Western Ontario and McMaster Universities (WOMAC) scale, Hospital for Special Surgery (HSS) score, Knee injury and Osteoarthritis Outcome Score (KOOS), Short Form 36 (SF-36), visual analog scale (VAS) and Knee Society pain scale are often used to quantify pain. However, knee adduction moment (KAM) can be used as a surrogate for knee pain as the magnitude of the moment is positively linked with pain [28]–[30]. Valgus knee braces help reduce the KAM by applying a counter moment using the three-point bending principle. KAM will be addressed in more detail in section 2.3.2. In addition to pain reduction, knee function improvement is a goal of OA management [57]. Multiple studies have confirmed the functional benefits of offloading orthoses. Some of these benefits include increased ability to walk, increased walking distance, increased activity, and decreased fall risk

[58]. Functional changes are typically measured in VAS, WOMAC function scale, time to pain onset during activity, and length of activity.

In a six-month study with 80 individuals with OA and an offloading orthosis, using a graded scale (0 = unlimited walking and 6 = less than 100m of walking), the mean walking distance score significantly improved from 4.23 ± 1.08 to 1.86 ± 0.68 over six months [58]. There was a significant reduction in pain from a mean of 6.25 to 4.18 as measured by VAS [58]. Patients also reduced pain medication by nearly half from a mean of 3.24 to 1.38 over the same period and increased knee function on the WOMAC scale [58].

Functional pain improvement during stair negotiation has been reported to improve in as little as one week. In a one-year study with the Ossur Unloader One Brace with seven patients, knee pain during stair negotiation and walking was significantly reduced at one week and at the four and 12-month follow-ups [59]. Difficulty performing daily living activities such as stairs was decreased at the four months follow-up and maintained at the 12 months follow-up as measured by VAS [59].

Pain often limits the amount of activities patients can tolerate. A one-year study with 18 patients examined offloading braces' effect on pain and if function improved with decreased pain symptoms [60]. Before bracing, patients reported moderate to severe pain averaging 7.3 ± 2.3 on the Cincinnati Knee rating system with daily activities. After bracing for nine weeks, the average pain score decreased significantly to 4.4 ± 2.1. At the one-year follow-up, nearly half of patients stopped using pain medications [60]. Walking distances was one of the measures used to quantify function, with 44% of patients reporting they could not walk more than three blocks and 22% reporting they could not walk a single block [60]. After nine weeks, all patients reported improvement, with only 28% reporting they could only walk three blocks [60]. There were no significant improvements in stair negotiation, running or jumping. However, some patients who were previously inactive began participating in swimming or bicycling activities [60].

2.3.2 Lower Leg Kinematics

Knee flexion and extension are reduced by pathological OA gait, but offloading orthoses have been reported to further impair patients' ROM. In a study of the Ossur Unloader One, the orthosis was compared to insole and exercise groups. There was a varus moment decrease of 5.5% sustained over the 12 months and increased gait speed with the brace [61]. Knee extension angle in the braced group was significantly impaired compared to exercise and insole groups. It gradually improved over time, but it did not reach the other groups' extension angles at 12 months [61]. Another study compared wedged insoles and an offloading brace and found some impairment in knee flexion in the braced cohort compared to the insole [62].

The knee adduction moment is high in patients with varus malalignment. Valgus knee braces provide an opposing moment, which reduces the net frontal moment at the knee joint, known as the varus moment or KAM. There are two main peaks of KAM during gait, the first at ~10-20% and the second at ~45-55% of the gait cycle. There are conflicting studies on whether knee braces reduce the load through the affected compartment and their effectiveness at increasing joint space. There is significant evidence however, that offloading orthoses decrease KAM [54].

A study of 10 individuals with OA examined the KAM with a knee orthosis in a 4° and 8° valgus inclination compared to a wedged insole of 4° [63]. The second peak KAM was reduced significantly by 18% and 21% for the 4° and 8° valgus inclination and 7% for the insole [63]. Knee adduction impulse was decreased in similar amounts [63]. The varus knee angle in the frontal plane was also reduced using all interventions, reducing the knee lever arm [63]. No significant changes were found between control conditions and braced conditions for ankle eversion moment and lever arm [63].

Biomechanical data of 16 patients demonstrated that after wearing an offloading brace for four weeks, there was a significant increase in walking speed and cadence [64]. Additionally, there was an increase in step length from the affected leg, while the contralateral leg showed a decrease. Finally, the knee brace contributed to an approximate 10% reduction in the knee varus moment [64].

Offloading orthoses have been shown to affect the kinematics of surrounding joints. The ipsilateral hip has a decreased adduction in the first half of the stance phase and a lower second peak

adduction moment [65]. The contralateral hip shows a lower first peak adduction moment, and the contralateral knee shows a slight increase in the knee adduction angle compared to unbraced conditions [65].

2.3.3 Analysis of Current Interventions

This section will review current offloading devices with supporting literature. It is not inclusive of all devices available on the market but provides an overview of the different conceived designs. Some designs, such as those specific to patellofemoral OA are not included, as this review concentrates on medial tibial femoral OA treatment.

There are two main frame types: single or double uprights. In a frame with a single pair of uprights, they are attached to the femur and tibia on the medial side of the leg. Attachments in a single upright are done solely through strapping. There are two pairs of uprights in a double upright design; they are placed on both the lateral and medial sides of the leg. In a double upright, the two sides are attached to form the rigid frame, with straps applied posterior to the femur and anterior to the tibia.

Offloading falls into three main categories, direct, indirect and distraction. In some designs to unload the joint, there is direct contact with the lateral aspect of the knee joint, usually through a pneumatic bladder or a telescoping condyle pad. Indirect offloading uses the mechanical joint to create vertical or angular displacement of the uprights to get the required varus angle for joint offloading. Another type of indirect offloading is when straps are used to produce the bending moment. A distraction brace combines valgus offloading with external tibial rotation.

Current orthoses have low daily use and low compliance rates due to discomfort, poor fit, and lack of perceived effect [56]. Orthosis designs also contribute to low compliance with patients complaining of size, thickness and weight of the orthoses [56].

DonJoy and Ossur are the top two studied manufacturers of OA offloading knee braces, and they both have extensive lists of designs [66]. The most studied designs were chosen to be presented.

Figure 2 shows the Ossur Unloader One, a single upright indirect offloading orthosis. It uses adjustable diagonal straps about the knee to apply the bending force from the frame. There is

minimal condyle pressure with this design, and the straps act as the anchor point instead of a condylar pad. The single upright sits alongside the affected compartment to open the compartment.

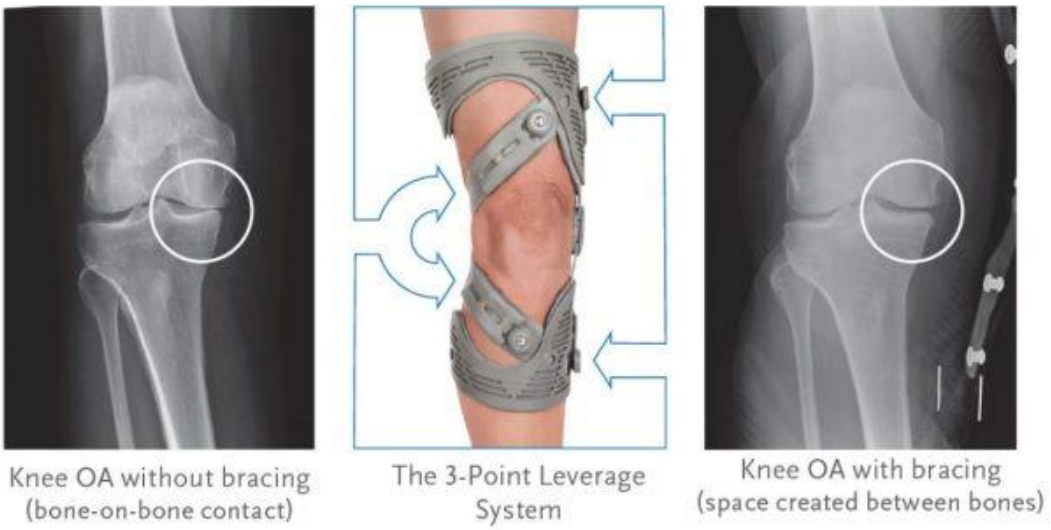

Figure 2: Ossur Unloader One with single joint and indirect offloading moment.[67]

The DonJoy OA Adjuster, as shown in Figure 3, is a double upright indirect offloading orthosis. The indirect offloading comes from adjustable screw joints on the contralateral upright located distally to the knee. The screw joints are manually adjustable with a tool, creating a deviation from the centerline of the upright, therefore increasing the bending moment of the brace.

Figure 3: DonJoy OA Adjuster orthosis. Adjustable offloading joints circled in blue on the right [68]

The strapping pattern helps stabilize the knee in anterior-posterior translations and adds additional friction points to help limit the movement of the orthosis on the user.

The PROTEOR OdrA shown in Figure 4 is the only distraction knee brace with supporting literature. The medial joint adds vertical separation during full knee extension through the physical vertical displacement of the top and bottom upright at the joint to offload the compartment. Simultaneously, the lateral joint causes a rotation of the tibia to reduce the lever arm to the KAM. Few studies have been completed on this brace, although results are promising, showing decreased pain, improved gait function and reduced pain medication [69]–[71].

Figure 4: PROTEOR OdrA distraction orthosis left [72], mechanism function on right [73].

However, one study did note a case of an adverse effect of lower-limb varices, and 25% of patients enrolled reported excessive pressure at the front of the tibia [70]. Another study noted that 13% of patients had withdrawn from the brace cohort due to cutaneous side effects [71]. This can be caused by excessive pressure from the orthoses and should be studied further to ensure patient safety. However, it is difficult to compare the comfort of braces, as many studies neglect to collect specific comfort information or reasons for withdrawal.

First patented in 1994, the development of the Generation II Orthotics joint marked a change away from using direct contact and can be seen in Figure 5. The Generation II Orthotics patent is separate from the Ossur Generation II brace. A competitor brace, the Bledsoe Thruster 2, was removed from the market in 2005 after a patent infringement case about the adjustable offload. This joint design allows for adjustment proximally to the knee joint, allowing for an increase of the moment with the femur and tibia straps.

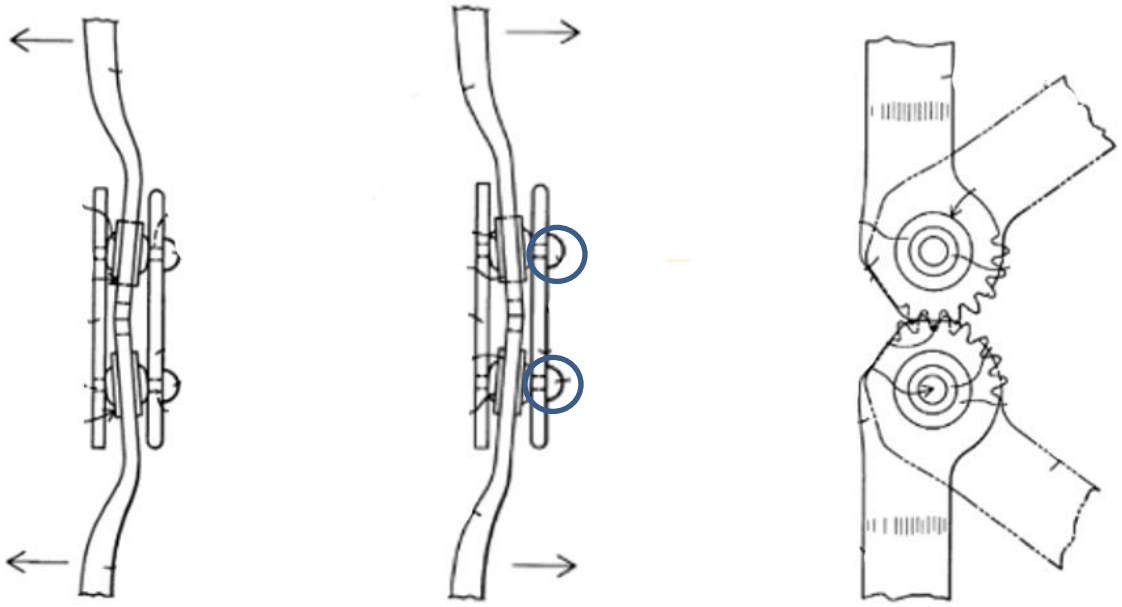

Figure 5: Generation II patented adjustable joint system. Labels are removed from patent images for clarity. Adjustable screws circled in blue in the middle image create an angular displacement of the brace uprights. [74]

However, there are some drawbacks. As indicated in the patent filing, the adjustment screws will need to be rotated equally to maintain proper alignment for the geared joint. Before the Bledsoe brace was removed from the market, one of the first 3D studies on condylar separation was conducted, comparing the amount of condylar separation achieved by various commercial offloading orthoses. The Bledsoe brace using this joint design was one of only two braces (the other being DonJoy OA Adjuster) that produced medial condyle separation consistently [74].

Townsend Industries presented another unique adjustment to offloading with their Rebel Reliever orthosis, shown in Figure 6. This is a double upright orthosis using indirect offloading with an adjustable telescoping upright. The slide and lock system is ipsilateral to the affected knee compartment. This length imbalance causes an angular shift that increases the force applied by the brace. The mechanism does not require external tools, unlike the previous joint.

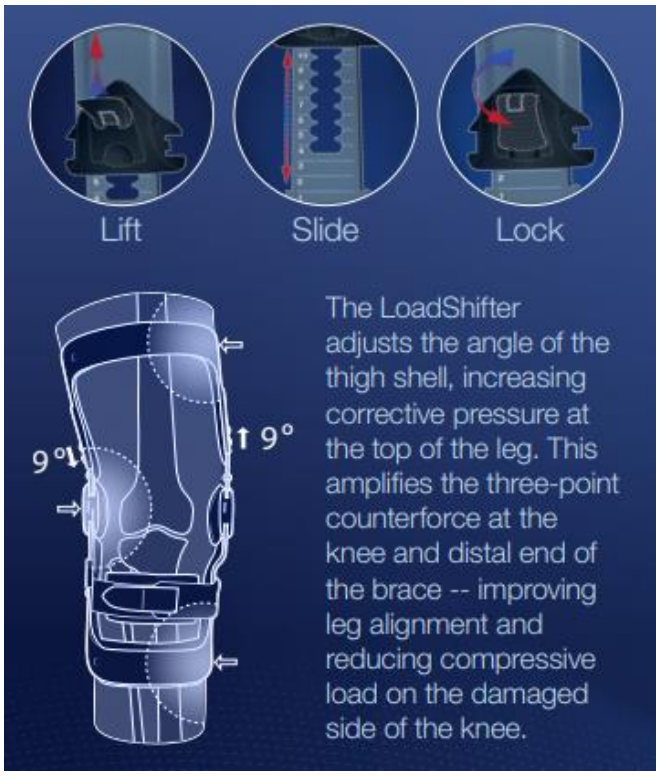

Figure 6: Townsend Rebel Reliever orthoses with unique adjustable offloading using the load shifter, a telescopic upright with a locking mechanism. The increased length on one side of the orthosis creates and intensifies the offloading force [75].

The majority of offloading braces use a geared joint design, as depicted in Figure 5 and Figure 9. The shape of the gear contact surface helps follow the knee condyles' natural movement, allowing for a more polycentric joint with rotation around a curved surface; the curve tapers towards extension, mimicking the shape of the condyle and the anterior-posterior motion of the knee. Finally, the gears serve another purpose- increased stability and ROM control. Increased stability comes from the flat surface at full extension, which limits hyperextension. The gear teeth are often used to help implement flexion and extension stops for rehabilitation purposes.

A unique joint design that differs from the current market offerings is from Breg. The Dynamic Unloading Osteoarthritis (DUO) orthosis is listed as the only dynamic offloading dual upright orthosis on the market [76]. The brace uses a cam follower to engage a pin in the last 30° of extension that causes an increase in the arc, a vertical separation between the top and bottom upright. This mechanism is shown in Figure 7. The magnitude of offloading is also altered by the adjustment screws changing the length of one side of the frame. This is depicted in Figure 7 and

is a similar mechanism to the Rebel Reliever. This additional brace adjustment would most likely be applying pressure through the entire ROM and increase in the last 30° of extension through the joint cam mechanism.

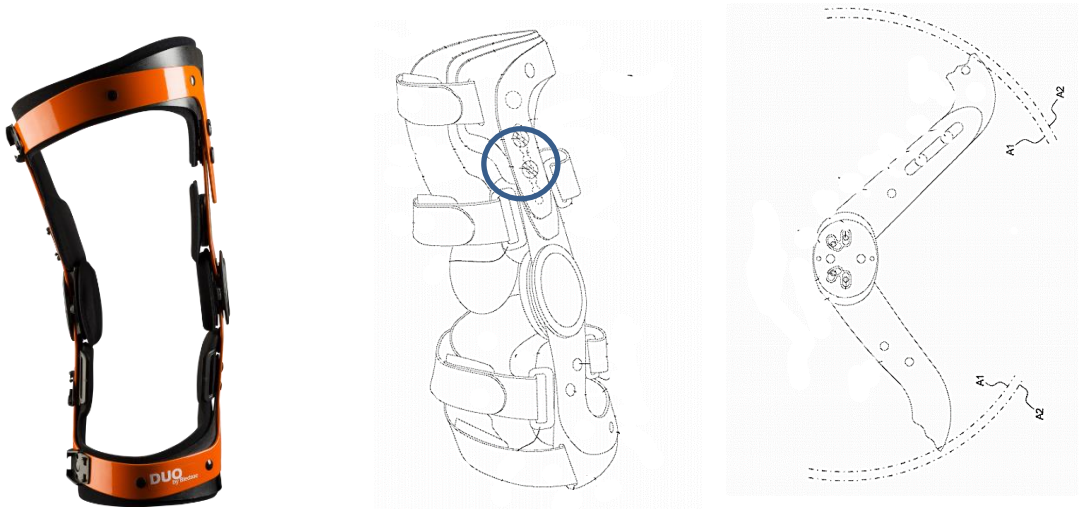

Figure 7: Breg DUO orthosis consumer model (left) [76]. The center and right patent images have labels removed for clarity [77]. The additional offload adjustment is identified with a circle in the center figure. The right figure depicts the functioning of the offloading cam joint. The brace follows the shorter A1 curve in flexion and is shifted to the longer A2 curve in extension.

Knee orthoses with passive assist are relatively new to the market and have less supporting literature. The OA Rehabilitator is an offloading knee brace combined with swing assist developed by Guardian, shown in Figure 8. The swing assist encourages proper heel-to-toe gait by applying an elastic force posteriorly to the tibia, thereby enabling extension. The orthosis has a double upright frame. The direct offloading is produced through an air bladder that inflates and applies pressure against the knee. The medial joint has an elastic that stores energy in flexion. The removable blocks depicted in Figure 8 are attached to the joint cover plate with screws and are used to offset the pivot point and vary the tension applied towards knee extension. Limitations of this device include manual adjustments and a bulky design. However, studies show that this brace may help increase quadriceps and hamstring strength over time in addition to the standard offloading orthosis benefits [78]–[80].

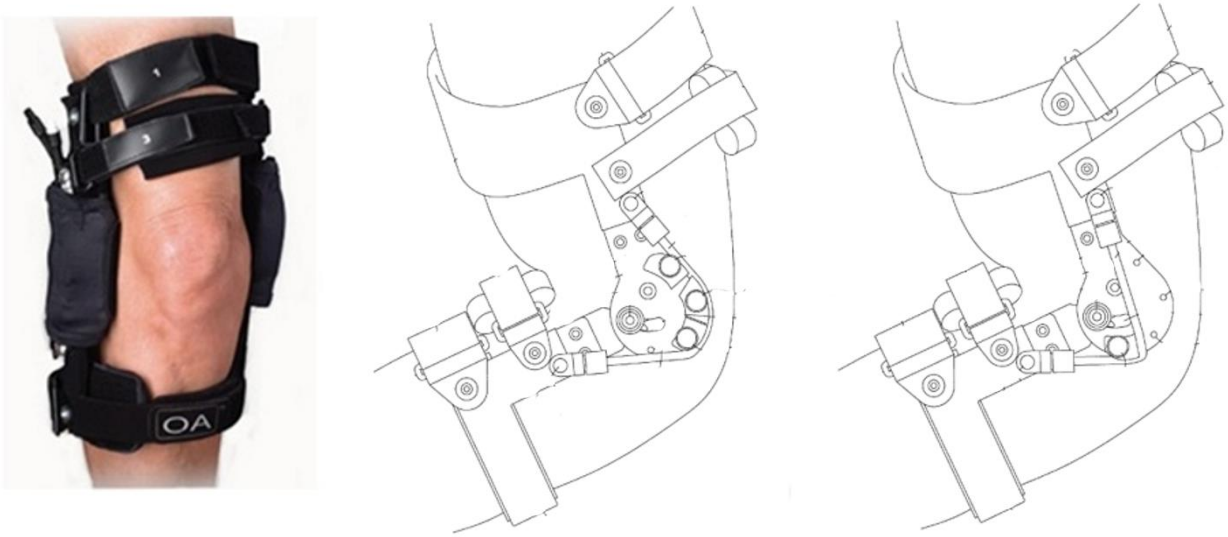

Figure 8: The OA Rehabilitator brace is a double upright, direct knee contact offloading brace with extension assist. The picture on the left depicts the consumer model [81]. The center and right images are derived from the patent and have labels removed to show the extension assist system more clearly, consisting of an elastic material and tensioning blocks mounted by screws [82].

The Levitation orthosis by SpringLoadedTechnology in Figure 9 uses a double upright brace that stores energy in flexion and releases energy in extension to assist with variable output through an adjustment screw. The orthosis can come with an optional pneumatic pad to provide better realignment and enhance offloading [83]. Therefore, this brace can directly offload by applying pneumatic pressure to the knee and can indirectly offload through the brace. A squat test study demonstrated a reduction in both quadriceps and hamstring activation [84]. These results may be contradictive of muscle-strengthening found in the previous assist orthosis.

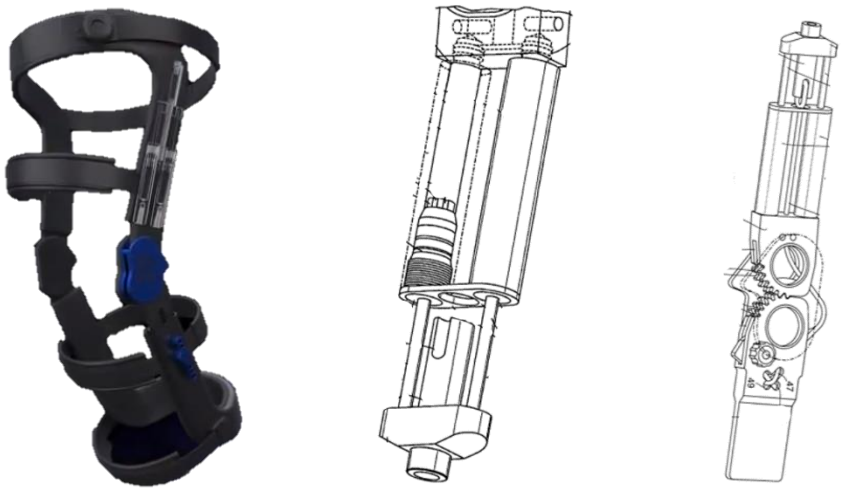

Figure 9: SpringLoadedTech Levitation knee orthosis commercial model (left) [85]. Patent images with labels removed for clarity in the center and right images show the spring cylinder system that controls the length of the cord attached to the lower upright [86]. Energy is stored in flexion and released to assist with extension.

2.4 Mechanical Models

This section summarizes techniques used to calculate the orthosis contribution to the knee moment and the biological KAM.

2.4.1 Orthosis Moment

The following section introduces techniques used to measure the bending moment, stiffness, and offloading moment of the orthosis.

2.4.1.1 Three-Point Bending Model

Many studies use a simplified three-point bending model to calculate the valgus moment of the orthosis. For single upright braces, the distal ends of the upright act as the supporting forces, and the center strap acts as the main applied force [51], [87]

The force diagram is demonstrated in Figure 10, where F_1 is the main applied force by the adjustable force strap, and F_2 and F_3 are the supporting counter forces [51].

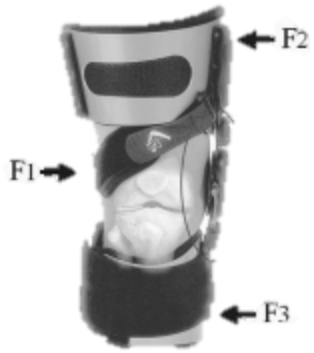

Figure 10: Three-point bending diagram of a single upright orthosis. The diagonal strap acts as the main applied force [51].

Single upright braces that use horizontal straps or rigid frames follow a similar model to the double upright, shown in Figure 11 [88].

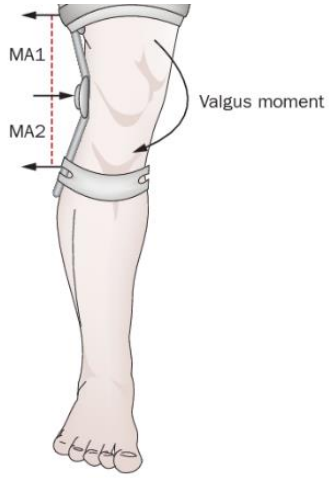

Figure 11: Three-point bending diagram for orthosis without a loading strap, where the supporting forces are at MA_1 and MA_2. The valgus moment applied by the brace is shown [88].

For double upright orthoses, a single upright, usually contralateral to the affected compartment, acts as a beam in three-point bending where the center joint acts as the main force. In contrast, the distal ends of the upright supply the supporting forces.

2.4.1.2 Stiffness

While the orthosis moment cannot be directly calculated using stiffness, it is an important mechanical property to consider when designing an offloading orthosis. The stiffness, *k*, is a function of the applied force *F* and deflection of the beam δ as shown in (2-1) [89].

$$k = \frac{F}{\delta} \tag{2-1}$$

Figure 12 depicts the force required to deflect current offloading orthoses by 0.5 in. Please note that the graph's title was cropped as it was erroneous compared to the accompanying methodology and description of the figure. The text writes 0.5 in, while the graph title displayed 0.05 in [90]. The author of the graph determined rigidity as a force of 15 lbs to compress the hinge by 0.5 in.

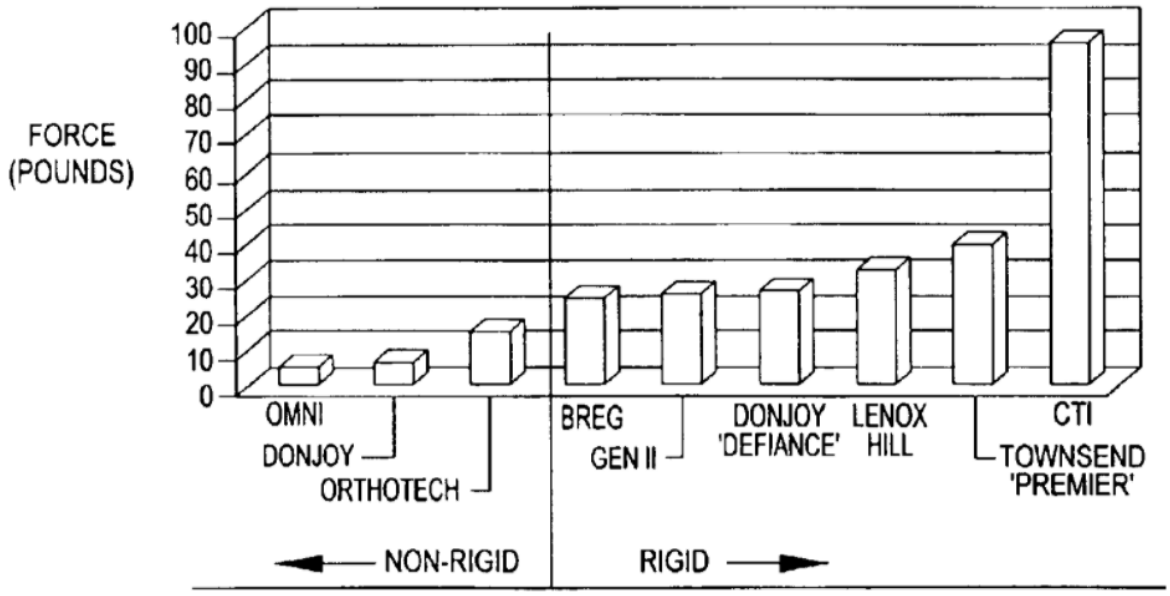

Figure 12: Force in pounds required to deflect offloading knee orthoses by 0.5 in at the joint adapted from [90]

The compression force for each brace from left to right is 5.4, 6.4, 14.8, 24.1, 26.6, 26.7, 32.2, 39.4 and 96.2 lbs, respectively [90].

2.4.1.3 Dynamics

Studies have shown that the magnitude of the counter moment is not always represented in the net knee moment [43], [50], [91]. Offloading orthoses are most effective at reducing the peak varus moments. However, they have a reduced effect at the beginning and end stages of gait, as shown in Figure 13, even with a constant or higher magnitude of valgus force applied by the brace, as shown in Figure 14. It is shown that there is a consistent drop in the valgus force around 20% of the stance phase, which is in the single support midstance. Variations in knee kinematics, possibly due to ligament and muscle stabilization during this part of the stance phase, may contribute to the drop in the measured valgus force. It is important to note that even though the valgus force decreased in Figure 14, it did not seem to have a marked increase in the varus moment at 20% stance in Figure 13.

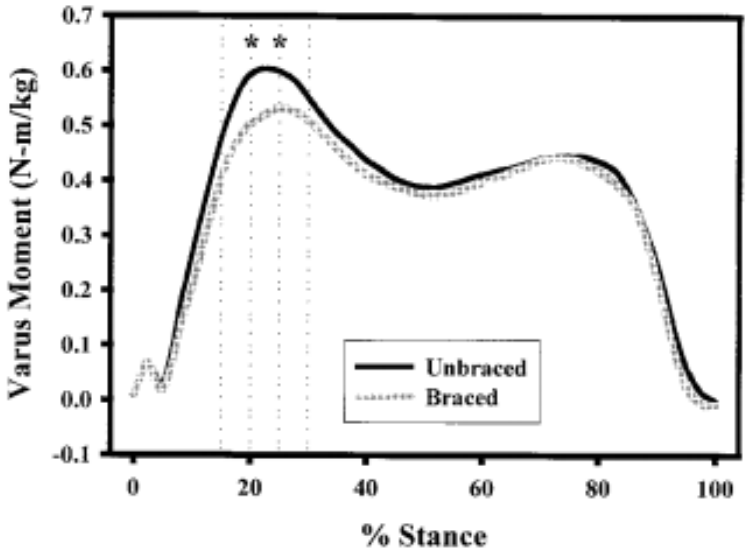

Figure 13: Mean varus knee moments in both braced and unbraced conditions of five knee individuals with OA during the stance phase [91].

When considering the effect of bracing, a simple sum of moments about the knee will not suffice as the moment delivered throughout the stance phase is not constant. Complete dynamic analysis of both unbraced and braced conditions is needed to determine the full effect of bracing on the KAM. See section 2.4.2.2 for more information on inverse dynamic analysis.

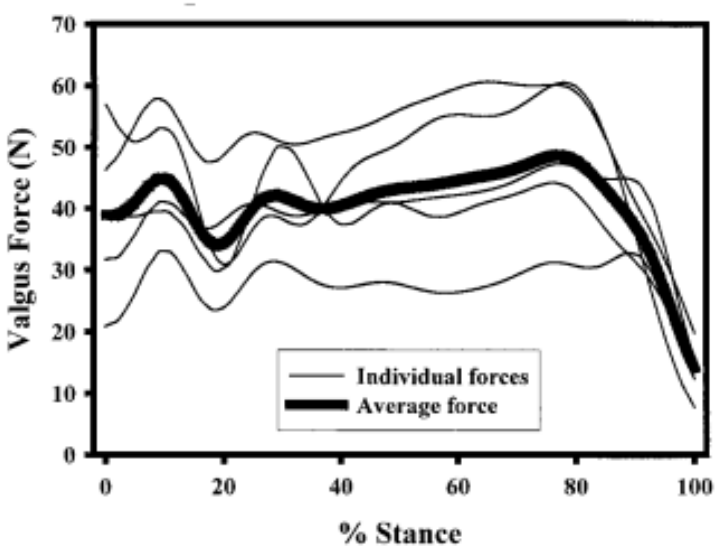

Figure 14: Valgus force applied by the brace for five individuals with OA, and the mean force is shown with the bold line during the stance phase [91].

2.4.2 Knee Adduction Moment

There are two main methods for calculating the knee adduction moment (KAM): the lever-arm method and inverse dynamics.

2.4.2.1 Lever-Arm Method

The lever-arm method has been shown to estimate KAM and KAM magnitude changes and is considerably faster than inverse dynamics [92], [93].

The lever-arm method is calculated as follows:

$$KAM = r \times GRF \tag{2-2}$$

In this approach, *r* signifies the frontal plane vector between the knee center and the center of pressure of the ground reaction force. The cross product of the lever arm *r* and the ground reaction force produces the magnitude of the KAM. Expanding (2-2) into its components gives (2-3) [92].

$$KAM = r_Y GRF_X + r_X GRF_Y \tag{2-3}$$

In the expanded lever-arm formula, r_Y is the vertical distance between the ground reaction force (GRF) center of pressure and the knee joint center and r_X is the medial-lateral distance between the GRF center of pressure and the knee joint center. The GRF is divided into its x and y components, represented by GRF_X and GRF_Y, respectively.

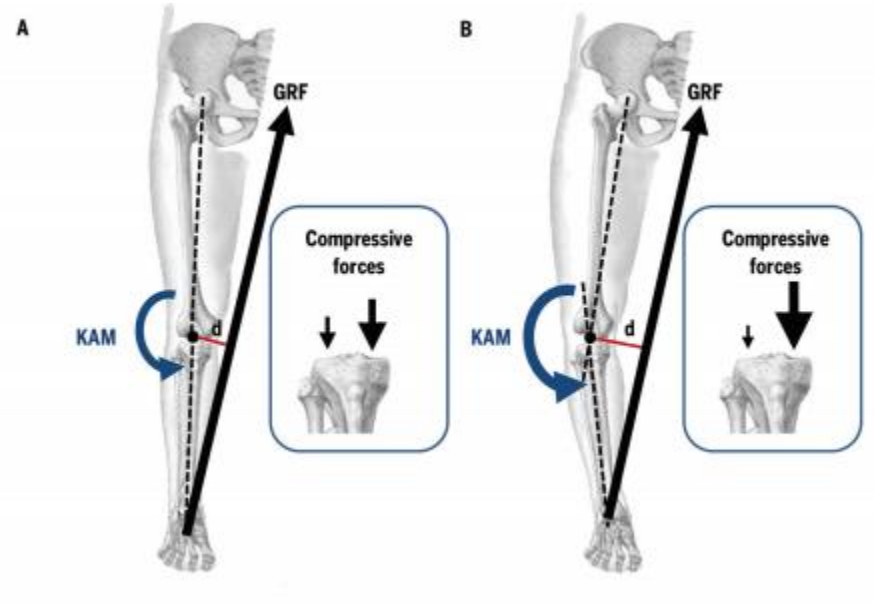

Figure 15: Lever-arm method diagram, the image on the left demonstrates a leg with a reduced varus angle, comparable to when wearing an offloading brace. The moment arm (d) is reduced. In the right image, the leg has an increased varus position, which increases the moment arm (d), therefore increasing the KAM and loading through the medial compartment [94].

This model relies on some assumptions. First, the angular acceleration of the shank must be zero; second, the calculated KAM moment is with respect to the laboratory frame, not an inner body or joint system; and third, the lower leg and foot act as a single rigid body. Thus, these assumptions work well for static standing calculations. However, these assumptions are invalid during gait, which can produce inaccurate outputs. Nevertheless, because it requires less data collection and is relatively easy to compute, it can be easily used by researchers who do not have access to all parameters needed to compute the inverse dynamics. Additionally, it can be beneficial in identifying changes in KAM under different conditions, keeping in mind that the magnitude of the moment will be flawed if calculated during gait [92], [93], [95].

2.4.2.2 Inverse Dynamics

Inverse dynamics is commonly used in laboratory settings to calculate the KAM. It is more accurate than the lever-arm method but requires additional computation. To calculate the KAM, subject-specific morphology information is needed in addition to segment kinematics, inertias, joint centers, segment and joint modelling equations and GRF. This method is frequently used in research and studies relating to gait analysis [93].

Inverse dynamics can be derived using Newton-Euler equations and link segment models. A variety of limb models exist, using different assumptions, such as frictionless hinge joints, rigid segments and mass location on the limbs themselves to aid in solving the equations. The recursive Newton-Euler approach to inverse dynamics has a linear complexity of O(n), where n is the number of bodies in the model [96]. Precise kinematics and external forces must be measured to calculate the body's kinetics. Motion capture systems record kinematic limb and joint data, while external force plates measure ground reaction forces during gait trials.

An example lower limb model used in inverse dynamics is shown in Figure 16. This figure demonstrates the movement in the sagittal plane, with joints indicated with a circle and rigid body segments with a line. The center of mass is marked with a point on each rigid body. External markers would be applied in the experiment at key joint areas; the head, hip, knee, ankle and toes. A force plate would capture the ground reaction force in gait.

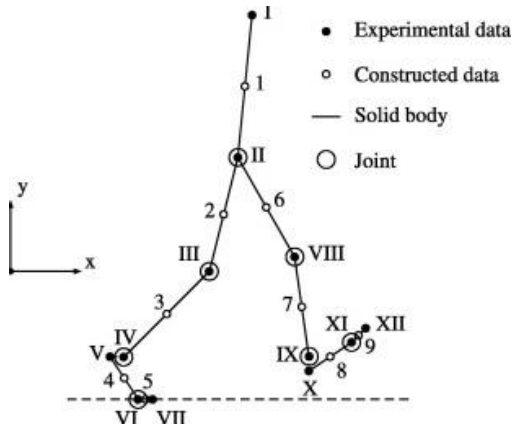

Figure 16: Example limb diagram used in inverse dynamics [97].

Chapter 3- Design

The aim of the design is to develop a variable offloading knee orthosis joint to improve patient comfort and perceived effect.

To guide and achieve optimal orthosis design, quantitative and qualitative factors have been identified for the design criteria of the variable offloading orthosis joint. The literature review has shown that current orthoses possess limited daily use and low compliance rates from patients. This is mainly attributed to discomfort, poor fit, and lack of perceived effect [56]. Orthosis designs also contribute to low compliance with patients complaining of excessive size, thickness and weight of the orthoses [56]. Therefore, the comfort, fit and perceived effect are of particular importance in the design criteria.

3.1 Design Process

Figure 17 demonstrates the design process used to develop and validate the proposed novel offloading joint. The previous literature survey and following design sections give detailed summaries of each step. First the problem was identified, low compliance of offloading braces due to lack of comfort and perceived effect, next a literature survey was completed. Design criteria were developed based on literature and the problem statement. A base design is created, followed by iterations and calculations to a final design, which is then mechanically validated.

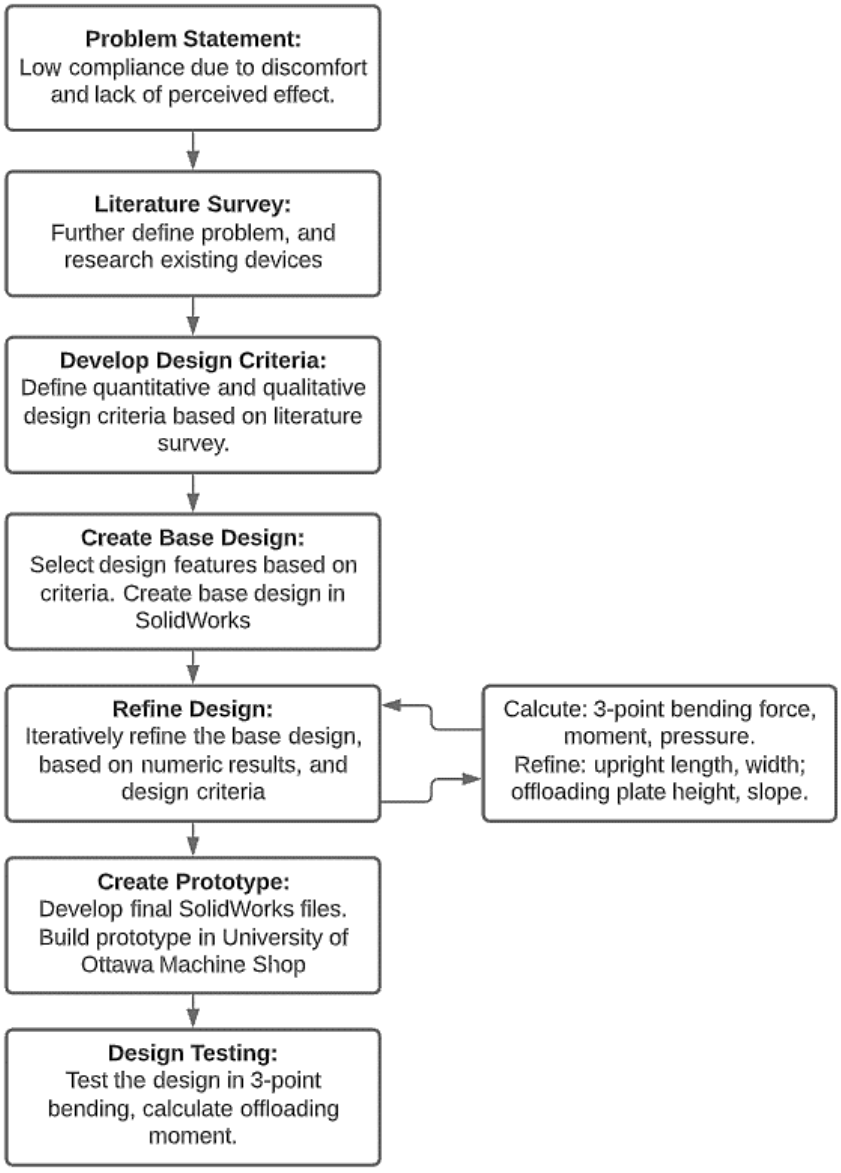

Figure 17: Design process flow diagram

3.2 Quantitative Design Criteria

The following criteria have been adapted from [98], with additional standards and benchmarks added through literature review. In this section, pressure, rigidity, comfort, ROM and offloading moment criteria are quantified.

3.2.1 Pressure

Figure 18 demonstrates anatomical areas that are critical while designing lower limb orthoses. These sites represent areas of movement, bony prominences, surface tendons, nerves and vessels. While it is impossible to avoid all these areas when designing a knee orthosis, like those indicated for movement, it is essential to consider them for design comfort.

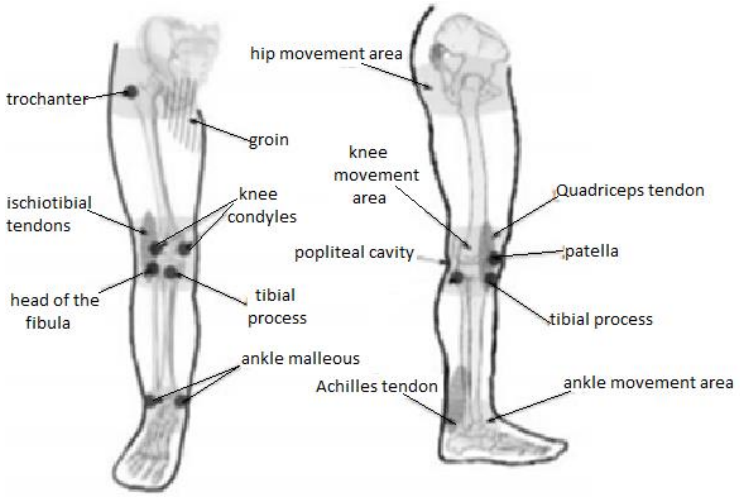

Figure 18: Areas to avoid while designing lower limb orthoses, amended from [99].

It is also recommended to take into consideration both the maximum pressure tolerance (MPT), the ratio between the applied force and the dispersion area, and the pressure discomfort threshold (PDT), the pressure limit where the patient would have uncomfortable sensations [99]. PDT is lower than Pressure Pain Thresholds (PPT); however, it is harder to measure than PPT as it is more variable between patients. Therefore, PPT was used for design purposes as described further below. MPT should be also be considered, as an increased surface area of force dispersion does not always result in less discomfort. It is recommended to design using critical force values and only increase surface area as needed to maintain overall patient comfort [99], [100].

MPT is approximately 9.9 kg/cm^2 (970.89 kPa) on the tibia for healthy patients [101]. PPT is estimated to be 6-11% of the average skin strength (7640 kPa) [99]. The lower end of the PPT in symptomatic knee OA in the patellar region has been estimated at 1.00 kg/cm^2 (0.75,1.32 CI 95%) [102]. The lower end of the range was chosen as it has been demonstrated that symptomatic OA is associated with lower PPT [102].

Ischemia is caused when blood flow is restricted and can be caused by external pressure. In the upper body, a blood pressure cuff induces ischemia about 30 mmHg [103]. A higher cuff inflation pressure of about 55 mmHg is needed in the lower limbs to cause ischemia [103].

To quantify pressure in this design, an assumption of constant force applied perpendicular to the surface area will be used. The pressure is calculated using (3-1), where *F* is the applied force, *A* is the surface area, and *P* is the pressure [104].

$$P = \frac{F}{A} \tag{3-1}$$

3.2.2 Rigidity

There are two main designs for rigid body offloading: single or double upright. Single upright designs often consist of a large solid body frame on both the thigh and shin to provide offloading. Alternatively, a single upright design can also have a solid body upright with two angled straps on superior and one inferior to the knee joint approaching the compartment to be unloaded. There are also two additional straps to maintain the position of the brace. Single-jointed knee braces often use inflatable bladders on the lateral side of the knee to adjust the corrective force applied [105].

The double upright has two sets of uprights; one set on the lateral side of the leg and one set on the medial side of the leg. There are fewer strap configurations with double joint designs. Most have two straps inferior to the knee, one proximal to secure the orthoses from slipping, and one distal for load application and dispersion. The distal strapping is often semi-rigid, whereas the proximal strapping is flexible. A flexible strap is also applied to the posterior side of the rigid anterior thigh frame and superior to the knee joint.

One study measured and compared the pressure distributions of single versus double upright braces and found a pressure point at the top lateral bar of the brace for both [106]. However, the single upright brace also had a pressure point on the medial lower part of the brace, whereas the dual upright had better pressure distribution [106].

When designing the offloading mechanism, while possible to unload using straps, it is best to use strapping solely to adjust the fit and stabilize the position of the brace. The position of the uprights produces better offloading results, has better displacement control, rigidity, durability and better soft tissue contact in comparison to strapping [107]. It has also been demonstrated that adjustments through the rigid frame of the brace have a more significant impact on valgus alignment than the tension of the straps [51].

Therefore, this variable offloading orthosis joint design will be operating under the assumption of integration into a double upright brace design because of the aforementioned pressure distribution and force application benefits.

As rigidity is a crucial component to the mechanical function of the orthosis, to quantify this criterion, a baseline stiffness comparison to existing devices will be completed using values from section 2.4.1.2.

3.2.3 Comfort

For the frame, the design must ensure that the orthosis fit is comfortable and has a slim profile that does not impede the movement of the user. This translates to a weight less than 1.25% of users' body weight and a thickness less than 30 mm [108]. As size and bulkiness are the main complaints from users, reducing thickness should increase comfort and compliance in orthosis use.

For the interface, due to the high forces required to create the bending moment, the rigid frame should have a surface area sufficiently large to distribute the forces at the brace-skin interface. Padding should also be applied, especially on bony contact surfaces, like the knee joint. A PPT of 1.00 kg/cm^2 must be respected.

3.2.4 Offloading

The brace should apply sufficient corrective force to unload the medial compartment. Current literature indicates an offloading moment ranging from 0.038 to 0.133 Nm/kg, with many sources reporting values around 0.05 Nm/kg [54], [91], [109]. To calculate offloading moment *M*, a relationship between the applied force, *F*, and the length of the beam is required. The internal bending moment is defined by (3-2.

$$M(x) = \frac{F}{2}x \tag{3-2}$$

The max bending moment is calculated using (3-3). The maximum bending moment is at the center of the beam, replacing *x* with *L/2*.

$$M_{center} = \frac{FL}{4} \tag{3-3}$$

3.2.5 Range of Motion

The minimal ROM requirement is to allow full knee flexion and extension. This is defined as 0° (extension) to 130° flexion [110]. Degrees of hyperextension should be limited to ensure better stability.

The offloading should be applied when needed during the gait cycle. Thus, to increase comfort and perceived effect, force should be applied for the knee flexion range of approximately 0° to 30°, as discussed in section 2.4.1. This eliminates unnecessary forces during high flexion positions, like sitting, thereby increasing patient comfort.

3.3 Qualitative Design Criteria

Durability, reliability, adjustability and safety are essential criteria for the design of orthoses. They are not restrictive and may not be quantified with the current project scope; however, they should be considered in the design process.

The orthosis should be affordable with low initial and maintenance costs. This can be achieved through proper material selection and modularity of the device to ensure that inexpensive components can be available.

The orthosis should be durable. It should offer a long-expected useful lifetime and have design considerations towards any environmental factors that may damage or inhibit proper functioning. This includes consideration towards water and dust; typical factors when wearing a knee brace in outdoor conditions. Wear of components and methods to mitigate that impact, such as material selection and design modularity, must also be considered.

The orthosis should have high reliability to ensure continued operation under normal conditions. These criteria would include normal, predictable and easy maintenance, as it aids with patient mobility.

The orthosis should be easily operable and adjustable by the user. This includes design customization, adjustability and user-centric design for ease of use.

Finally, the design must be safe and limit harm to the user or individuals nearby. This would include precautions such as implementing pinch guards and reducing sharp geometry.

3.4 Design Criteria Summary

Table 1 summarizes the design criteria contained in section 3.2 to 3.3. The goal of the design is to increase compliance using variable offloading to enhance comfort and perceived effect, as well as generating a perceivable offloading moment. The design should be modular to help reduce costs, and keep the design adjustable to the user's preference and comfort.

Table 1: Summary of main design criteria

Design Criteria	Definition	Values
Comfort		
Variable Offloading	Offload the joint in stance when it is needed most, and reduce offloading in swing when it is not needed.	Offload: 0°-30° flexion Reduce offload: 30°-130° flexion
Thickness	Keep device thin, to increase comfort and reduce interactions with clothing	Maximum: 30 mm thick
Weight	Keep device lightweight for comfort.	Maximum: 1.25% of users body weight
Pressure	Pressure must be below PPT	1.00 kg/cm^2
Perceived effect		
Offloading moment	Generate a sufficient offloading moment for a perceivable effect	0.038 to 0.133 Nm/kg
General		
Range of motion	Allow for full normal range of motion of the knee	0°-130° flexion
Safety	Pressure should be below ischemic threshold	55 mmHg
Modular	Modular, adjustable design. Little to no tools required.	N/A

3.5 Computer Aided Design

When a knee orthosis is attached to a patient's leg, the joint is stationary at the knee joint center, and the uprights are secured to the thigh and calf. Thus, the joint itself can be used as a reference point to the knee center and the uprights as reference points for the upper and lower limb segments. The flexion and extension of the knee are represented by the rotation of the limb segment reference points with respect to the joint. Therefore, the varying magnitude of the offloading with respect to flexion angles can be achieved within the joint of the orthosis. With this concept, several conceptual designs were achieved and evaluated using the qualitative and quantitative criteria of comfort, pressure, rigidity, range of motion and offloading moment. Subsequently, a final design was created using Computer-Aided Design. Full drawings have been omitted due to patent investigations.

The design was developed in SolidWorks and is depicted in Figure 19. The assembly consists of two beams with a gear joint style interface, and the joint allows for 0° to 130° of flexion. These beams form the orthosis upright. The geared interface mimics the condylar aspect of the knee joint, increasing comfort compared to a traditional hinge joint that flexes around a pivot point.

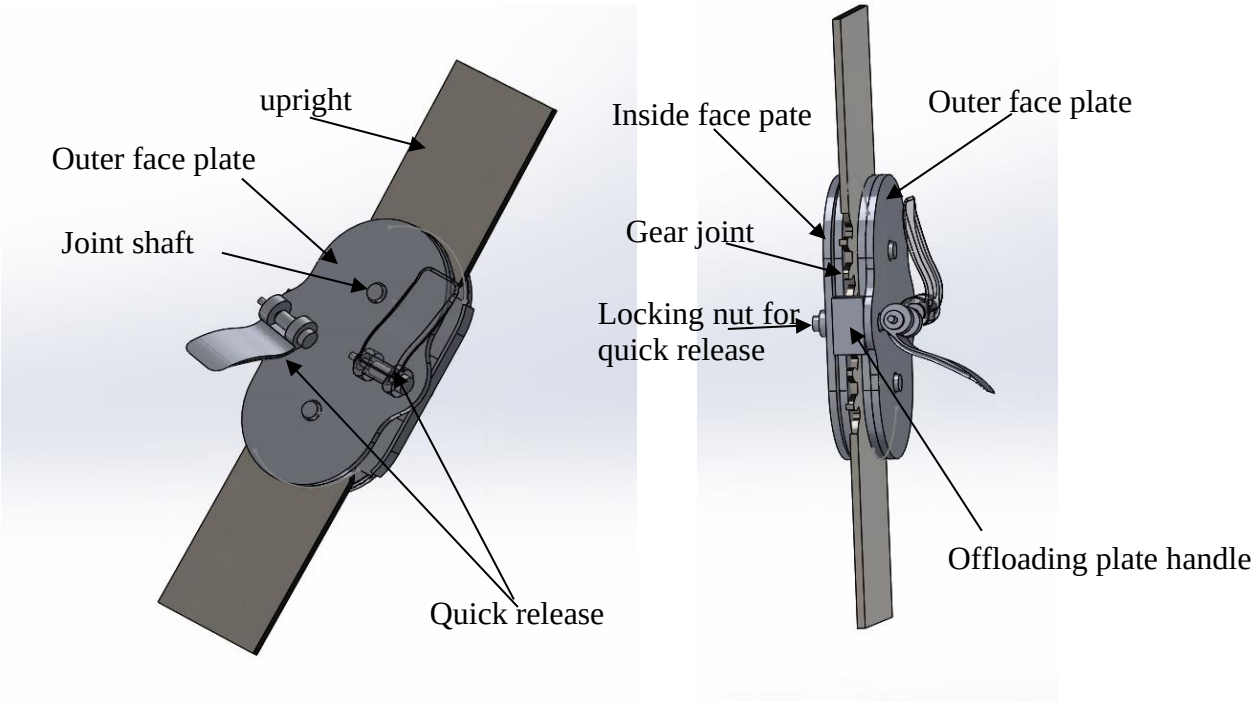

Figure 19: SolidWorks design of offloading joint with faceplates

To achieve the condylar shape, radii of lateral condyles were used to create the curve for the geared knee joint, as the design would be placed on the lateral side of the leg to offload the medial joint. The medial condyle is elliptic in shape, with approximately 9 mm difference between the two radii in the ellipsis [111]. The lateral condyle is much more round in shape and has a near-constant single radius of curvature between 10° and 160° flexion [112], [113]. Thus, a 20 mm constant radius circular spur gear was chosen for the joint to help mimic the shape of the femoral condyle.

To address the comfort and pressure criteria, a pad would be applied on the inside faceplate. The pad is mounted using holes that line up with the locking nut and can be easily pulled off and reapplied by the user for cleaning.

With the rigidity criteria, the upright will produce the offloading moment. Using the upright will result in better displacement control and soft tissue contact, among other benefits discussed in 3.2.2. In addition, the pressure points listed in 3.2.1 can be avoided by using the upright instead of strapping or telescoping pads which would cross the motion area of the biologic joint and apply direct pressure on bony prominences.

An angular displacement will be introduced within the joint from 0° to 30° of flexion to produce the variable offloading moment. The displacement of the beams at the joint center will produce a horizontal displacement between the beams and the leg of the user at the attachment points. Attaching the uprights to the leg of the user will create the bending moment required to offload the biological joint. To create the angular displacement at the joint, offloading plates will be used.

The offloading plates are shown in Figure 20. The offloading plate possess a raised profile to push against the upright from 0° to 30° of flexion, creating the angular displacement needed to achieve the joint offloading moment. A plate with the opposing profile makes contact with the other face of the upright to help guide the angular movement. The two plates are joined together with a handle. They have a channel for the quick release bolts and for the bearings that support the uprights. To improve modularity and usability, a quick release was implemented. The quick-release mechanism uses pressure to lock and unlock the offloading plates in place and was chosen

as it does not require tools. This separates it from many braces currently on the market, which require screwdrivers, Allen keys, or specialized tools to change offloading settings.

The channels allow the user to slide the plate into the orthosis joint. The profile of the offloading plate can be adjusted in height and curvature to better suit different offloading magnitudes and ranges of motions associated with different activities. The modularity of the plates satisfies the adjustability and durability criteria outlined in 3.3. For example, if the user needed a greater offloading moment, an offloading plate with a high profile can be slid into place. The modularity can also support easy repairs and changes as required, making it a durable design.

The plate profile in Figure 20 shows a plate explicitly made for use in gait, where the offloading profile is applied in 0° to 30° of flexion. The offloading joint sits at the centerline of the knee. It is assumed that the orthosis would be a proper fit and maintain its centerline joint position. The static position of the orthosis joint allows for the calculation of flexion and extension from the centerline of the knee.

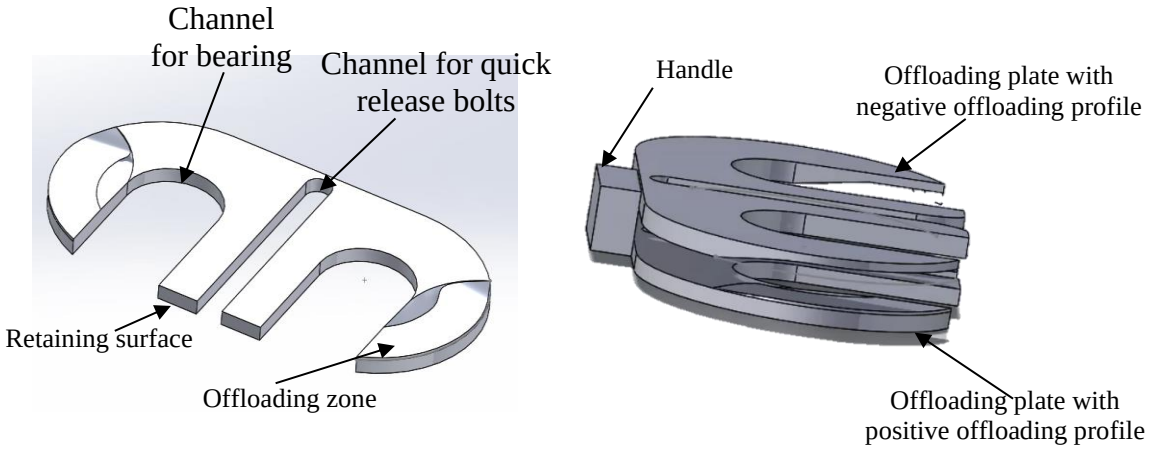

Figure 20: Left image depicts one side of the offloading plate for use during gait. The profile engages the upright in the last 30 degrees of extension. The image on the right is the complete offloading plate assembly with the handle and plates.

The plates are attached to the handle with internal pins. The distance between the plates is equal to the thickness of the upright. Increasing the height of the offloading profile would increase the magnitude of offloading by increasing the available deflection distance. Increasing the length of

the curvature of the offloading zone would increase the range of motion where offloading is applied.

Figure 21 and Figure 22 show cut-away views of the joint mechanism. The uprights contain spherical bearings which allow movement along the shaft that is attached to the rear faceplate. The uprights can pivot with respect to their axis of rotation. The spherical bearing was chosen as it can take loads in multiple directions, which is necessary due to the movement of the brace, and forces applied for offloading. The pivot from the spherical bearing is necessary to support the angular displacement introduced by the offloading plate.

Shown in Figure 21 is the offloading plate in position against the retaining wall of the faceplate. The offloading plates slide into the mechanism, using the spherical bearing channels to align with the joint shafts. The offloading plate is fully inserted once it rests against the retaining wall. Once inserted, the quick release can be pushed down and locked into place. This additional pressure reduces the space between the offloading plate and the faceplate and retains the offloading plate in place.

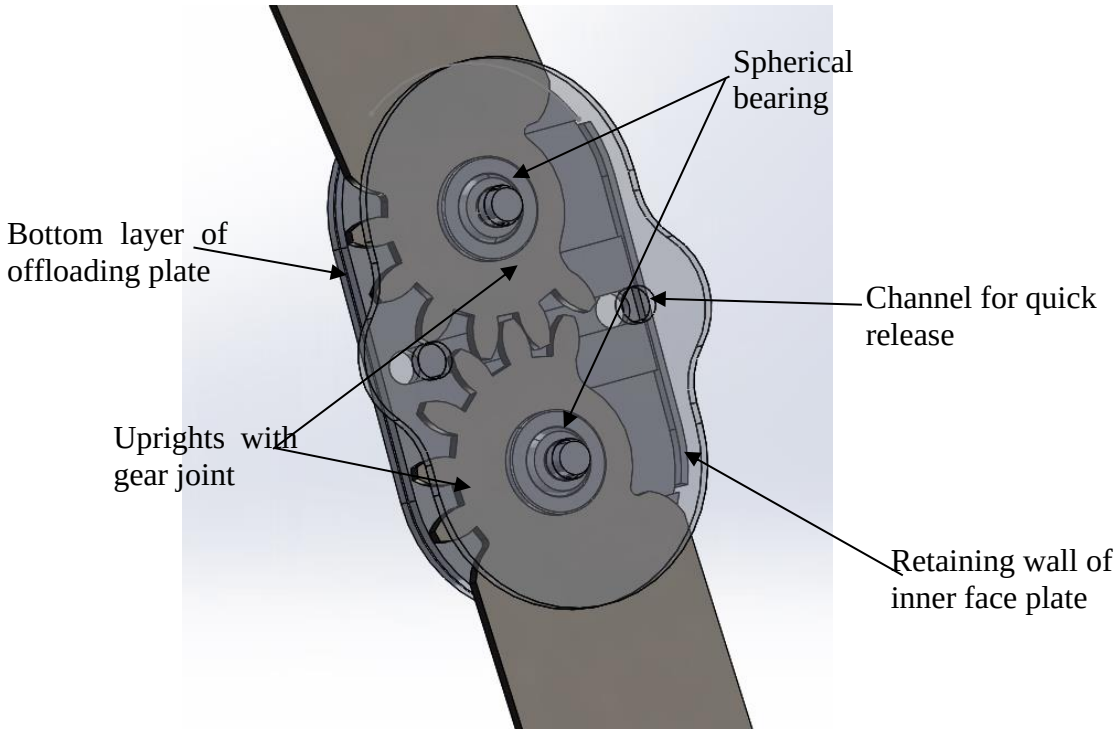

Figure 21: Joint with transparent faceplate and an invisible top layer of offloading plate, showing gear joint uprights, spherical bearings, and bottom of offloading plate. Quick-release mechanism not pictured.

The offloading plate is shown entirely in place in Figure 22. The bearing's outer ring is flush with the upright, and the inner sphere of the bearing protrudes to a point between the surface of the upright and the thickness of the offloading plate. The channels in the offloading plate help guide the user in sliding in the plate, help maintain the position of the plate, and allow for bearing movement. The offloading plates have a rectangular handle that the user can hold to change the plates.

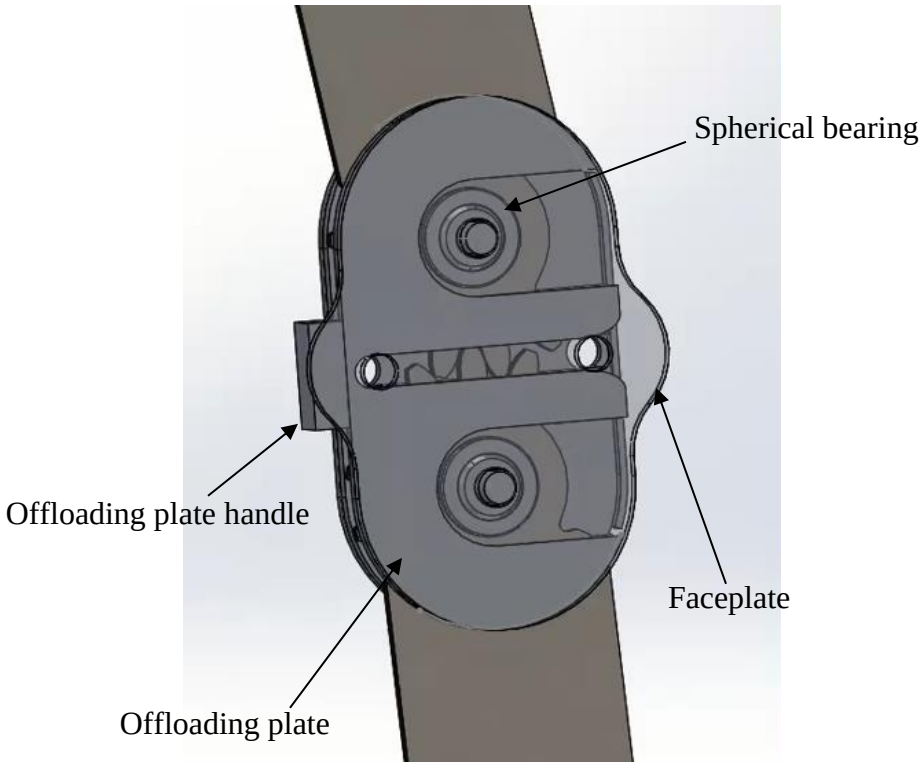

Figure 22: Joint mechanism with transparent faceplate, pictured with the full offloading plate. Quick-release not pictured.

3.5.1 Prototype Development

An experimental prototype was developed to validate the design shown in section 3.4. To begin the prototype process, an average OA patient is selected for anthropometric data. The median age of knee OA diagnosis is 55 years, and OA is more prevalent in females than males [23]. The average US mass for a female of 55 years old is approximately 80 kg [23],[114]. This, combined with an average height of 162 cm, gives a BMI of 30.5, consistent with the overall OA population that tends to be overweight or obese [23],[114].

Next, estimates from existing designs were used to create baseline stiffness values for deflection and material identification. More detailed information for the stiffness measures can be found in section 2.4.1.2. Assumptions for stiffness estimates include constant profile and homogeneous material.

Given the size of an average patient and using the base measurement from off-the-shelf braces, 15 cm per upright arm was chosen. Thus, the total beam length would be 30 cm. This distance passes the head of the fibula and the ischiotibial tendons listed in 3.1 [115], [116].

The estimated stiffness values with the varied materials and the standard upright length were used to estimate the minimum and maximum forces required to achieve the bending moment defined in section 3.1 of 0.038-0.133 Nm/kg. Equation (3-3) is used to calculate the bending moment range forces. These forces were then used to calculate a constant pressure over a typical knee pad surface area of approximately 0.00375 m^2 (7.5 x 3.5 cm). The pressure was compared to ischemic and PPT values as defined in section 3.2.1 using (3-1).

An example calculation of an iteration in the design process is presented below. To start, the force range is found based on the literature values of perceivable offloading moment. Equation (3-3) is modified, where M_{min} is replaced with the minimum offloading moment from the perceivable range, L represents the total length of the beam, and F_{min} is the force required to produce the minimum moment, shown in (3-4). The maximum and minimum forces found are 141.87 N and 40.53 N, respectively. Below is a sample calculation.

$$M_{min} = \frac{F_{min} L}{4} \tag{3-4}$$

$$\left[0.038\ \frac{Nm}{kg}\right] * 80\ kg = \frac{[F_{min}] * (2 * 0.15m)}{4}$$

$$[F_{min}] = 40.53\ N$$

Next, with the force range calculated, the pressure is calculated based on the approximate knee pad surface area. The knee pad area is not directly applying pressure to the knee, as the design uses the uprights and deflection at attachment points to create the moment instead of strapping or a telescoping knee pad. This step is to approximate the pressure if there is a contact. The contact at the attachment points would be half of the pressure, as it is half of the force according to the three-point bending principle depicted in section 2.4.1.1.

Using (3-1) and replacing *F* with the force required to achieve the minimum bending moment F_{min}, with *A* the approximated knee pad area, and P_{min}, the pressure caused by the force required for the minimum bending moment. The maximum and minimum pressures calculated with (3-5) are 37832 Pa and 10808 Pa, respectively. Below is a sample calculation.

$$[P_{min}] = \frac{[F_{min}]}{A} \tag{3-5}$$

$$[P_{min}] = \frac{[40.53\ N]}{0.00375 m^2}$$

$$[P_{min}] = [10808\ Pa]$$

Next, the total required deflection was estimated from the forces and stiffness values from 2.4.1.2. The results are shown in Table 2. The total deflection was compared to available bearing types to ensure angular allowance could be mechanically supported.

Table 2: Summary of approximate stiffness and required displacements of brace uprights.

Brace	**Material**	**Approximate Stiffness** (Nm/Deg)	**Displacement** (mm)	
			Low	High
Bregg	Aluminum	0.62	4.17	14.55
Gen II	Aluminum	0.69	3.78	13.19
Defiance	Reinforced Carbon Composite	0.69	3.76	13.14
Lennox Hill	Duraluminum	0.83	4.15	14.51
Townsend Premier	Solid core carbon graphite	1.016	2.55	8.91
CTI Ossur	Laminated carbon composite	2.48	1.04	3.65

With the base results, the design iterations with the selected material are achieved. The maximum offloading plate height was calculated from the required deflection and refined using the bending model described later in Chapter 4-. The maximum offloading profile height and the upright width were used to calculate the slope needed to get from the high profile of the offloading plate to the low profile with no offloading. Additional considerations from section 2.4 were also applied to

determine the beginning and endpoints of the slope. The greatest possible adduction moment reduction occurs at the beginning of stance phase from full extension to knee flexion less than 30°.

The brace needs to generate a moment between 3.04 and 10.64 Nm with the selected patient, calculated using the weight and moment values from 3.2.4. Considering the beam length, the force required to obtain this moment is between 40.53 N and 132.41 N. Both force values are below the PPT; however, the maximum load is severely over the ischemic limit. Therefore, the brace design iterations begin at the lower end of the force spectrum as ischemia will be more manageable.

The intended design does not directly apply force to the knee and uses the uprights as mentioned in 3.2.2. However, as joint swelling is a common symptom associated with OA and brace migration may occur, it is still important to consider safe force application.

3.5.2 Material Selection

Aluminum 6061 was chosen for all components due to its elasticity, density, availability and low cost. The uprights require elasticity to be able to perform its offloading function. Moreover, the overall weight of the joint and uprights is minimized by using aluminum. The principal alloying elements of silicone and magnesium make it resistant to corrosion, ideal for indoor and outdoor use of the brace. The mechanical properties of Aluminum 6061 are presented in Table 3.

Table 3: Mechanical Properties of Aluminum 6061 [117].

Property	**Value (**MPa)
Ultimate tensile strength	310
Tensile yield strength	276
Modulus of Elasticity	68900

3.5.3 Final Prototype

SolidWorks drawings and assembly files were used to manufacture a prototype for mechanical testing. The uprights and faceplates were made from aluminum sheet metal, and an aluminum block extrusion was cut to size and manufactured for the handle and offloading plates. Two GE 5 E spherical bearing were purchased and press-fit into each upright. This bearing allows for up to a 13° angle and approximately 4.25 kN of axial force, which is significantly greater than loads required for this use [118]. A CNC machine at the University of Ottawa machine shop was used for all other pieces.

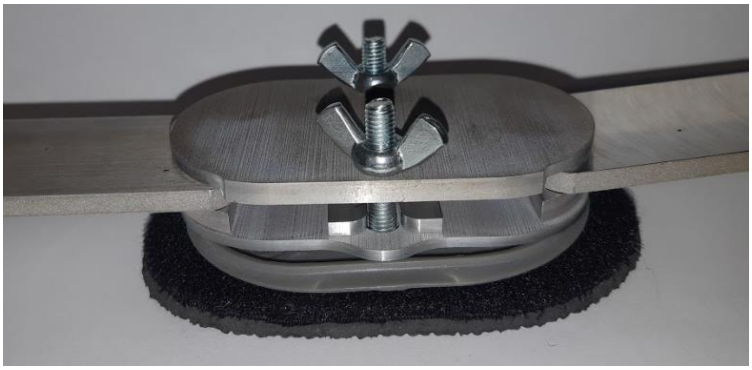

Figure 23: Manufactured prototype with a machine screw and wing nut. A plastic piece with fittings for the bolt heads with foam was added to demonstrate how it could be used against the knee joint.

The offloading plates were connected to the handle piece using pins. For the prototype, two 10-32 machine screws and wing nuts were using instead of quick release as they were more readily available, as shown in Figure 23. The coefficient of friction between two aluminum surfaces is high at 1.05; thus, minimal pressure is required to hold the plate in place [119].

An interior view of the joint is shown in Figure 24. The movement of the uprights seemed slightly restricted by possible friction points. If further cyclical testing is pursued, it is suggested to add Teflon on contact surfaces of the uprights. This is what is currently done in many offloading orthoses to reduce friction between the uprights and other metal contact surfaces.

Figure 24: Interior view of the joint with faceplate, pad, machine screws, and wing nuts removed. The photo shows the press-fit spherical bearings in the uprights, the offloading plate, and the faceplate.

All hole tolerances were 0.55 mm. Gear and bearing press fit tolerances were determined by the University of Ottawa machine shop. Bolts and butterfly nuts were purchased from a hardware store .

Chapter 4- Modelling and Simulation

This chapter presents the mechanical bending model developed for the novel variable offloading joint. The model uses a modified beam bending equation to calculate the predicted bending of the uprights under the applied three point bending force.

Once the model, boundary conditions and constants are developed, the model is then simulated under a force of 45 N. The results of the simulation are then compared to experimental results.

4.1 Modeling

To model the deflection in bending, a relationship between the applied force and beam geometry is required. Using Euler-Bernouilli beam equation (4-1), the deflection is a function of the resultant bending moment *M(x)*, the modulus of elasticity *E*, and the moment of inertia of the beam *I* [120].

$$\frac{d^2y}{dx^2} = \frac{1}{EI}M(x) \tag{4-1}$$

The bending moment diagram and the x and y coordinate system are shown in Figure 25. In the case of an orthosis, the beam is the upright supporting the bending moment. Using the force equilibrium, the reaction forces at the extremities are equal to one-half of the applied force.

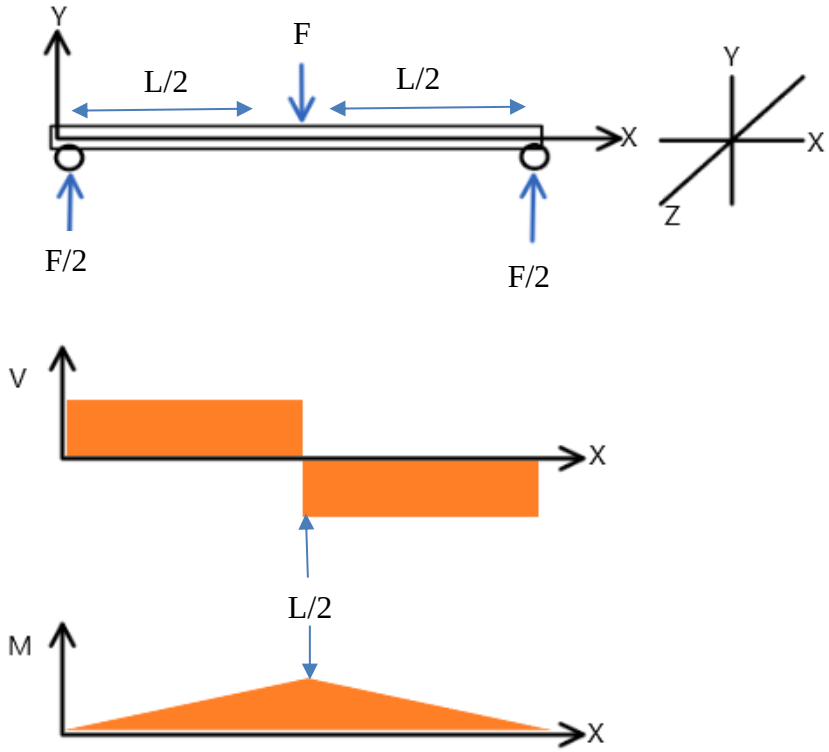

Figure 25: The top image represents a three-point bending experiment with applied force F at the center of the beam and reaction forces at the extremities located at half-length (L/2) from the X-axis center of the beam. The center image demonstrates the derived shear diagram. The bottom image is the derived moment diagram.

The internal bending moment as a function of *x* is calculated with (4-2).

$$M(x) = \frac{F}{2}x \tag{4-2}$$

The max bending moment is calculated using (4-3). The maximum bending moment is at the center of the beam, as shown in Figure 25.

$$M_{max} = \frac{FL}{4} \tag{4-3}$$

The moment of inertia for rectangular beams is calculated using the depth *d* and the width of the beam *w* with (4-4) [121].

$$I = \frac{d^3 w}{12} \tag{4-4}$$

A deflection model was derived from (4-1), where the deflection of a standard beam in three-point bending with a constant moment of inertia is defined. The proposed design incorporates the joint as part of the bending mechanics, altering both the inertia along *x* and the deflection through the offloading plate. The deflection of the uprights can be modelled from the beam tangent defined in (4-5):

$$\theta = \int_0^L \frac{M(x)}{E * I(x)}\, dx \tag{4-5}$$

where *L* is the length of the beam, *M(x)* is the moment as a function of the length, *E* is the modulus of elasticity, and *I(x)* is the moment of inertia as a function of length.

Equation (4-5) was used as the base equation to develop the mechanical model for the prototype offloading design. The prototype is symmetrical, and the model can be mirrored under the proper boundary conditions to represent the entire length of the prototype. The coordinate system and sectioning for the inertia function are shown in Figure 26. Section 1 of the model consists of a thin aluminum upright. Section 2 of the model is half of the joint assembly, and it is assumed to be a solid rectangular piece. As shown in Figure 26, the three-point bending force is applied at the center of the prototype model. The *x* coordinate system begins at the edge of the upright, and the *y* coordinate is a function of *x* and begins at the center of the prototype.

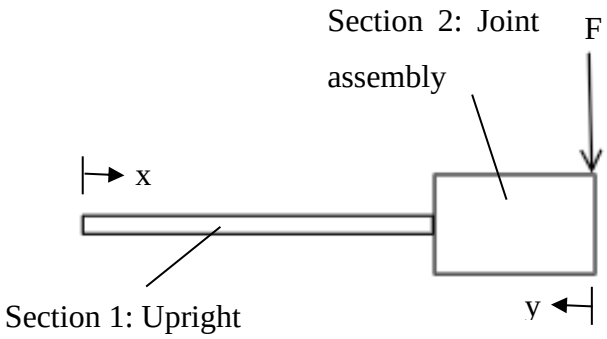

Figure 26: Diagram of coordinates and sectioning used to create the deflection model.

The moment of the beam is defined by (4-6) and is a function the applied force, *F*, fixed length of the model *L*, and the variable length *x*.

$$M = F(L - x) \tag{4-6}$$

The inertia for sections 1 and 2 are calculated with their respective depth, *d*, and width, *w*, values; shown in (4-7). The inertia equations can be represented as a piecewise function where they are constant over section 1 and section 2, respectively.

$$I_1 = \frac{{d_1}^3 w_1}{12} \quad , \qquad I_2 = \frac{{d_2}^3 w_2}{12} \tag{4-7}$$

Substituting (4-6) and (4-7) in (4-5) and integrating with respect to *x* for section 1 and *y* for section 2, the tangent formulas are found. An example integration for section 1 is shown in (4-8).

$$\theta = \int \frac{M(x)}{E * I(x)}\, dx = \frac{FLx}{EI_1} - \frac{FLx^2}{2EI_1} + C1 \tag{4-8}$$

Equation (4-8) is then integrated again with respect to *x* to obtain the deflection formula (4-9).

$$\delta = \int \theta = \int \frac{FLx}{EI_1} - \frac{FLx^2}{2EI_1} + C1\, dx \tag{4-9}$$

$$\delta = \frac{FLx^2}{2EI_1} - \frac{FLx^3}{6EI_1} + C1x + C2$$

To solve for the constants, boundary conditions must be applied. The boundary conditions at the section change must be equal to each other in all four formulas (tangent and deflection for both sections) to keep continuity.

Two models can then be developed based on changes to boundary conditions. The first model uses the continuity boundary conditions mentioned above (x_1 y_1). At the supported end (x_0), the boundary condition is that there is no deflection, and at the center of the beam (y_0), there are zero degrees of deflection. This would represent the typical beam bending scenario, however taking into account that most braces have additional material around the center of the beam holding the joint together, shown in section 2 of Figure 26, where less deflection, due to the increase in inertia would be likely to occur.

Compared to the first model given by (4-10), the second model represented by (4-11)is more accurate to the design of the prototype. The continuity boundary conditions are applied in addition to the extremity boundary conditions of zero deflection at the supported end of the beam (x_0). Next, the slope of deflection at the join of section 1 and section 2 (x_1, y_1) are equal to the tangent of the slope of the offloading plate (α). A third short section was inserted at the center of the beam (x_2, y_0), where *F* is applied to add the additional boundary condition of no slope of deflection at the center, which otherwise would have over-defined the model with just the two sections. Using these boundary conditions for the models in MATLAB, the integration constants can be solved for both Model 1 and Model 2 shown in (4-10) and (4-11), respectively.

Model 1:

$$\theta_1 = \frac{Fx(2L-x)}{2EI_1} - \frac{Fx_1(2L-x_1)}{2EI_1} - \frac{Fy_0(2L-y_0)}{2EI_2} + \frac{Fy_1(2L-y_1)}{2EI_2}$$

$$\theta_2 = -\frac{Fy_0(2L-y_0)}{2EI_2} + \frac{Fy(2L-y)}{2EI_2}$$

$$\delta_1 = \frac{Fx_0(I_2{x_0}^2 - 3I_2Lx_0 - 3I_2{x_0}^2 + 6I_2Lx_1 - 3I_1{y_0}^2 + 6I_1Ly_0 + 3I_1{y_1}^2 + 6I_1Ly_1}{6EI_1I_2} - \frac{Fx(I_2x^2 - 3I_2Lx - 3I_2{x_1}^2 + 6I_2Lx_1 - 3I_1{y_0}^2 + 6I_1Ly_0 + 3I_1{y_1}^2 - 6I_1Ly_1}{6EI_1I_2} \quad (4\text{-}10)$$

$$\delta_2 = \frac{Fy(-y^2 + 3Ly + 3{y_0}^2 - 6Ly_0)}{6EI_2} - \frac{Px_1(-{x_1}^2 + 3Lx_1 + 3{y_0}^2 - 6Ly_0)}{6EI_2} + \frac{Fx_0(I_2{x_0}^2 - 3I_2Lx_0 - 3I_2{x_1}^2 + 6LI_2x_1 - 3I_1L{y_0}^2 + 6I_1Ly_0 + 3I_1{y_1}^2 - 6I_1Ly_1}{6EI_1I_2} + \frac{Fy_1(3I_2{x_1}^2 + 3I_1{y_0}^2 - 3I_1{y_1}^2 - I_2{y_1}^2 - 6LI_2x_1 - 6LI_1y_0 + 6I_1Ly_1 + 3I_2Ly_1}{6EI_1I_2}$$

Figure 27 demonstrates the plot of the mechanical model of the beam in three-point bending with two sections demonstrated with (4-10) using a force of 45 N slightly higher than the estimated value from section 3.5.1. The plot illustrates the bending deflection of section 1 of the beam, which intersects curve 2 at the interface of sections 1 and 2. Section 2 plateaus at the center of the beam to 0 slope of deflection.

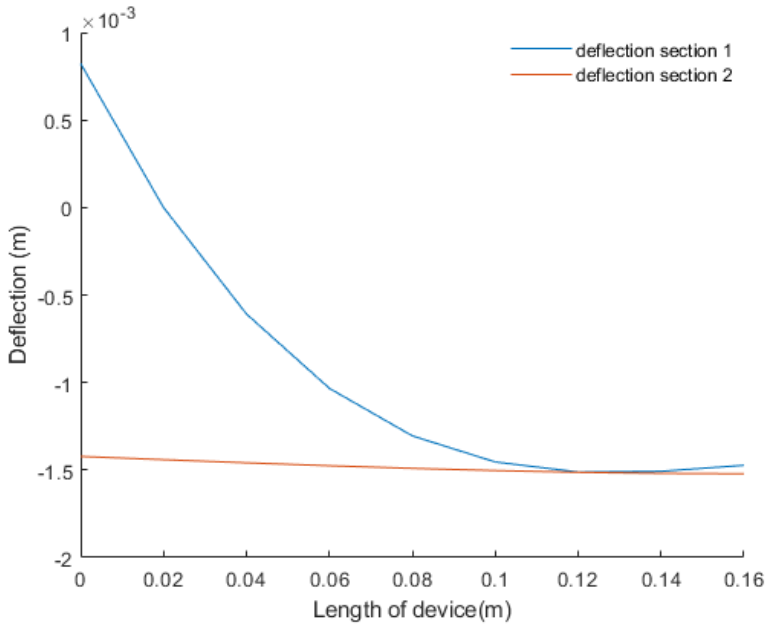

Figure 27: Mechanical model of the deflection of a beam in three-point bending in two sections as shown in Figure 26.

The following shows the development of the three-section mechanical model.

$Model\ 2$:

$$\theta_1 = \frac{Fx(2L-x)}{2EI_1} - \frac{Fx_1(2L-x_1)}{2EI_1} - \alpha$$

$$\theta_2 = -\frac{Fy_1(2L-y_1)}{2EI_2} + \frac{Fy(2L-y)}{2EI_2} + \alpha$$

$$\theta_3 = \frac{Fx(2L-x)}{2EI_2} - \frac{Fx_2(2L-x_2)}{2EI_2}$$

$$\delta_1 = \frac{x_0\left(Fx_0{}^2-3LFx_0-3Fx_1{}^2+6FLx_1+6EI_1\alpha\right)}{6EI_1} - \frac{x\left(Fx^2-3LFx-3Fx_1{}^2+6LFx_1+6EI_1\alpha\right)}{6EI_1} + \frac{x_1\left(-2Fx_1{}^2+3LFx_1+6EI_1\alpha\right)}{6EI_1}$$

$$\delta_2 = \frac{x_0\left(Fx_0{}^2-3LFx_0-3Fx_1{}^2+6FLx_1+6EI_1\alpha\right)}{6EI_1} + \frac{y\left(-Fy^2+3LFy+3Fy_1{}^2-6LFy_1+6EI_2\alpha\right)}{6EI_2} - \frac{y_1\left(2Fy_1{}^2-3LFy_1+6EI_2\alpha\right)}{6EI_2} \tag{4-11}$$

$$\begin{aligned}\delta_3 = {} & \frac{x_0(Fx_0{}^2 - 3LFx_0 - 3Fx_1{}^2 + 6FLx_1 + 6EI_1\alpha)}{6EI_1} \\ & + \frac{y_0(-Fy_0{}^2 + 3LFy_0 + 3Fy_1{}^2 + -6LFy_1 + 6EI_2\alpha)}{6EI_2} \\ & - \frac{x_1(-2Fx_1{}^2 + 3LFx_1 + 6EI_1\alpha)}{6EI_1} - \frac{y_1(2Fy_1{}^2 - 3LFy_1 + 6EI_2\alpha)}{6EI_2} \\ & + \frac{Fx_2(-2x_2{}^2 + 3Lx_2)}{6EI_2} + \frac{Fx(-x_2{}^2 + 3Lx + 3x_2{}^2 - 6Lx_2)}{6EI_2}\end{aligned}$$

Figure 28 demonstrates the three deflection curves of the mechanical model for the proposed design. The upwards direction of deflection in section two represents the slope caused by the offloading plate at section 1 and section 2 interface, which opposes the deflection of the upright. Curves 1 and 2 meet at the interface of sections 1 and 2. The deflection of section 3 defines the 0 slope boundary condition at the center, which is typical behaviour of a beam in three-point bending and meets curve 2 at the midpoint of the beam. The plot was evaluated using a force of 45 N.

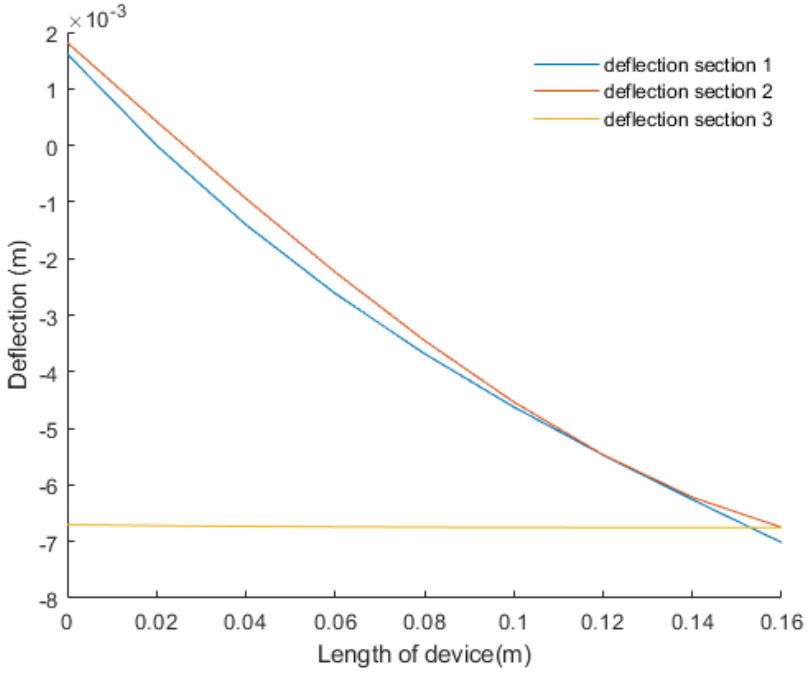

Figure 28: Plot of the mechanical deflection model for the prototype (Model 2).

4.2 Simulation

The first few iterations of the design process used an estimated stiffness of aluminum to obtain appropriate dimensions of the uprights to ensure correct deflection and moment generation required to offload the knee. The need for a mechanical model began with those first iterations.

Three models were introduced in the previous section: a general model, prototype model 1 (4-10), and a refined prototype model 2 (4-11). The three models were used to simulate the deflection of the proposed design using a force of 45 N in three-point bending and were then compared to experimental deflection values. The generalized model uses the base Euler-Bernouilli equation, assuming constant inertia and no specialized boundary conditions. The simulated deflection is shown in Figure 29.

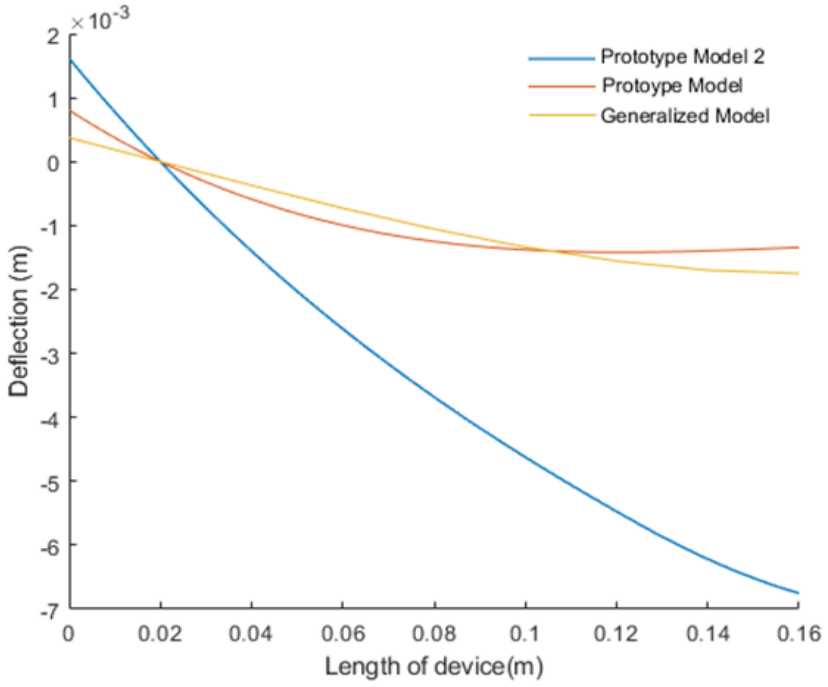

Figure 29: Comparison of three mechanical methods for calculation of the deflection of the upright.

Figure 29 shows the three different methods used to characterize the beam deflection. The graph is representative of one side of the prototype, as the prototype is symmetrical. The models can be reflected at the midpoint of the beam (x=0.16 m) to represent the entire prototype. The models were translated to align to x=0.02 m, as shown later in the next chapter, the 3-point bending supports were placed 0.02 m from the end of the beam experimentally.

Prototype Model uses (4-10). It results from a piecewise function, with zero deflection at the center of the beam and zero displacement at the supported end. As demonstrated in Figure 29, both the generalized model and prototype model have similar behaviours, and both severely overestimated the stiffness of the prototype, as shown in Table 4. The prototype model differs from the general at the boundary between sections 1 and 2, where section 2 has greater inertia, therefore, less deflection.

Prototype Model 2 is depicted in blue and uses (4-11). This model is also piecewise; however, it has the slope of the offloading plate as one boundary condition and a third condition at the center of the prototype, as described in the previous section. This mechanical model predicts the stiffness with greater accuracy compared to the other two more general models. The summary and comparison of these results are shown in Table 4.

Table 4: Comparison of methods to obtain the stiffness of the prototype.

Method	**Force (N)**	**Deflection (mm)**	**Stiffness (N/mm)**
Experimental	45	7.95	5.58
Prototype Model 2	45	6.75	6.63
Prototype Model	45	1.4	32.14
Generalized Model	45	1.75	25.71

Full details of the experimental results are found in the next chapter. The prototype was tested in three-point bending in full extension up to a force of 45 N. The stiffness was obtained by dividing the applied force by the measured deflection.

The Prototype Model 2 represents the experimental results well compared to the other methods and can be used in the future to assist with the development of other offloading plates.

Chapter 5- Experimental Results

The prototype was mechanically tested in three-point bending to determine the bending offloading moment. A custom testing rig was built to support the two extremities in various flexion angles. Testing was completed in the University of Ottawa Materials Lab.

This chapter also presents the results of the experimental testing, and demonstrates the analysis, and graphical representation of the device stiffness and offloading moment.

5.1 Experimental Set up

A three-point bending experiment was conceived to validate the variable offloading orthosis joint prototype mechanically. This test allows for data collection used to verify the offloading properties of the joint as defined in section 3.1 and the deflection model presented in Chapter 4.

The design prototype was manufactured at the University of Ottawa Mechanical Engineering Manufacturing Center and tested using the Instron 4482 Universal Testing Machine with the 100N load cell. Figure 30 demonstrates the experimental setup.

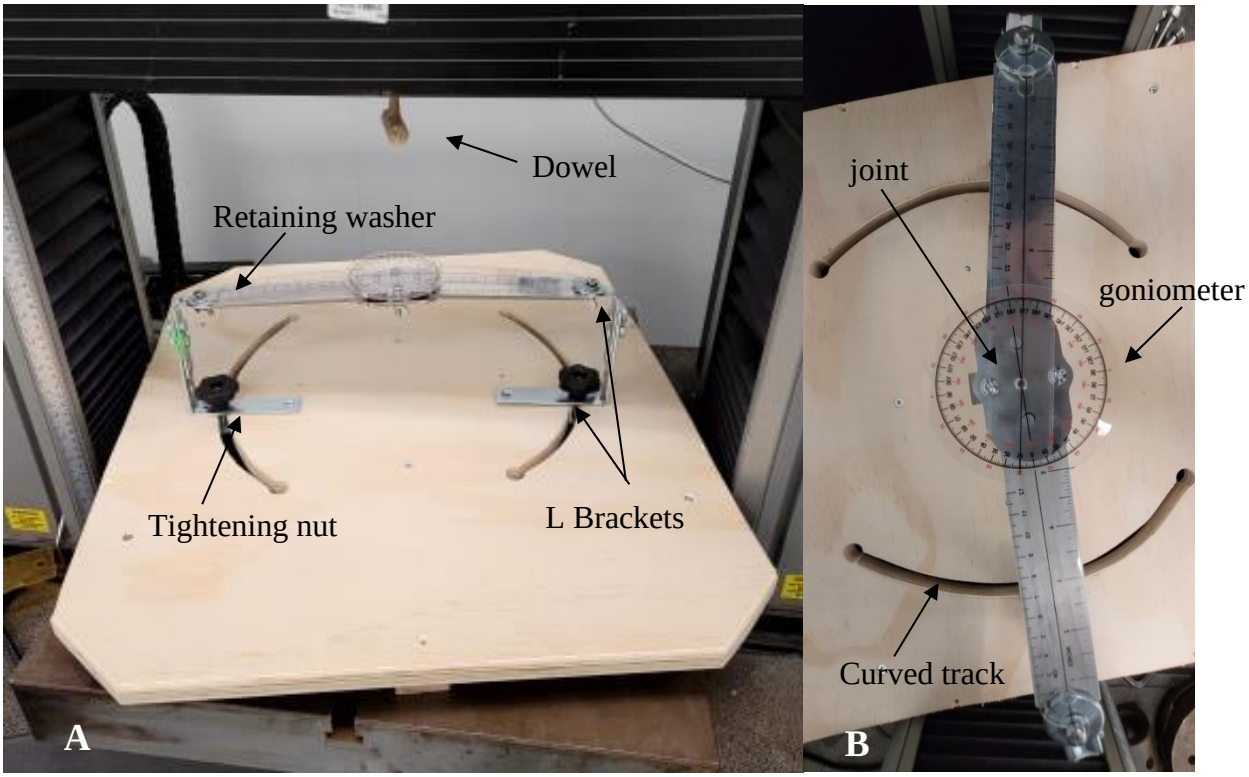

Figure 30: Three-point bending platform. A) the platform in the Instron machine, with brace mounted, and goniometer applied. B) overhead view of the testing set up. The curved track allows for flexion of the uprights with respect to the joint.

The platform shown in Figure 30 is composed of 1.9 cm thick plywood supported with 5.1 x 5.1 cm pieces of wood on the Instron base. The wood beams under the platform provide space for a tightening nut to allow motion of the brace between trial sets.

Two steel L-brackets were bolted together to create the three-point support at the extremities of the brace joint. A washer and bolt combination holds the uprights in place. The extremities of the L-bracket supporting the uprights were bent away from the brace to create a gap and not make contact with the upright while the experiment is in process. Thus, the main point of contact between the brace and the support is at the retaining washer.

The L-brackets are fixed to the plywood platform by tightening the nut and bolt. The bolt can move along the curved track, which is used to flex the brace joint. The nut and bolt fixation is tightened at each angle to maintain the position through the three trials. The goniometer was used to measure the flexion angle before each trial and was removed prior to the force being applied.

As shown in Figure 30, a wooden dowel was inserted into the 100 N load cell and fixed in place with a pin. A second dowel was attached perpendicularly to the first by screw. The screw is recessed into the dowel. The point of contact between the load cell and the joint is through the curved surface of the dowel.

The Instron was set to the configuration for three-point bending to mimic typical loading conditions for the brace. A new method was created on the BlueHill Universal software to slowly apply the load at a 6 mm/min rate until the uprights and joint were straightened, mimicking the tightening of the upright straps against the leg. Then, the load was gradually reduced to 0 N and returned to the origin before repeating two additional times for each testing angle.

The brace was tested at 5° flexion intervals as measured with a goniometer (shown in Figure 30B) between 0° (full extension) and 35° flexion. After the 35° flexion, the uprights are at the straightened (no angular displacement) position and would not have any further deflection. The range of 0° to 35° was chosen as it represents the profile of the offloading plate. 0° to 20° is where the uprights are engaged with the high offloading profile, and a constant angular displacement is applied. From 20° to 30°, the profile of the offloading plate is reduced using a slope, resulting in a steady reduction of angular displacement. At 35°, it is constant with no offloading profile. The 35° test represents the joint when it is not undergoing any displacement that would result in an offloading moment.

Figure 31(a) demonstrates the starting point of the three-point bending experiment, where the dowel is in contact with the brace joint. The angular displacement of the uprights from the offloading plate can be seen in the image.

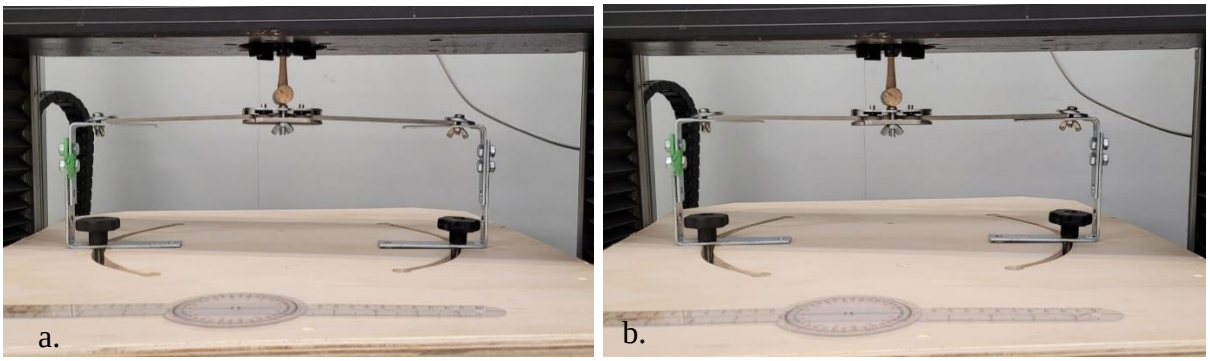

Figure 31: Experimental testing of the joint in three-point bending initial setup, shown in full extension. a. shows the dowel first making contact with the joint. b. shows the joint in a loaded and horizontal position.

Figure 31(b) demonstrates the end of a trial where the dowel loads the variable offloading joint. The deflection of uprights caused by the applied force brings the brace uprights and joint into a flat, horizontal position. This would be the equivalent of a brace user attaching the two supported ends to their leg.

5.2 Three-Point Bending Results

Using the experimental protocol described in the previous section, experimental data were collected from 0° to 35° in 5° intervals. The data was captured using the BlueHill software, and the results were exported to .csv files to be analyzed (see Appendix A. Raw Graph Data). All calculations and graphing were done in Matlab 2019a.

Linear regression was applied to the experimental data for all three trials for each graph. To verify the suitability of linear regression for modelling the relationship between the force and deflection of the beam, the mean linear regression was plotted on the same graph.

The flexural stress of a beam in three-point bending with a rectangular cross-section given by (5-1) must be less than the elastic yield point of aluminum.

$$\sigma_f = \frac{3FL}{2wd^2} \tag{5-1}$$

As determined in section 3.4, a minimum force of approximately 45 N is required to meet the minimum perceivable bending moment. Using the average dimensions of the prototype and the force of 45 N, flexural stress of 50 MPa was obtained. This is much lower than the material yield of 276 MPa. Thus, a linear model was appropriate to use as the material has not reached the stage of plastic deformation.

For each angle, three bending trials were recorded, plotted and the average linear fit was calculated. Figure 32 demonstrates an example plot of the three bending trials and the linear fit of the joint in full extension. The R^2 value of 0.997 suggests a good linear fit to the experimental data. The linear fit also demonstrates a low RMSE of 0.755 N.

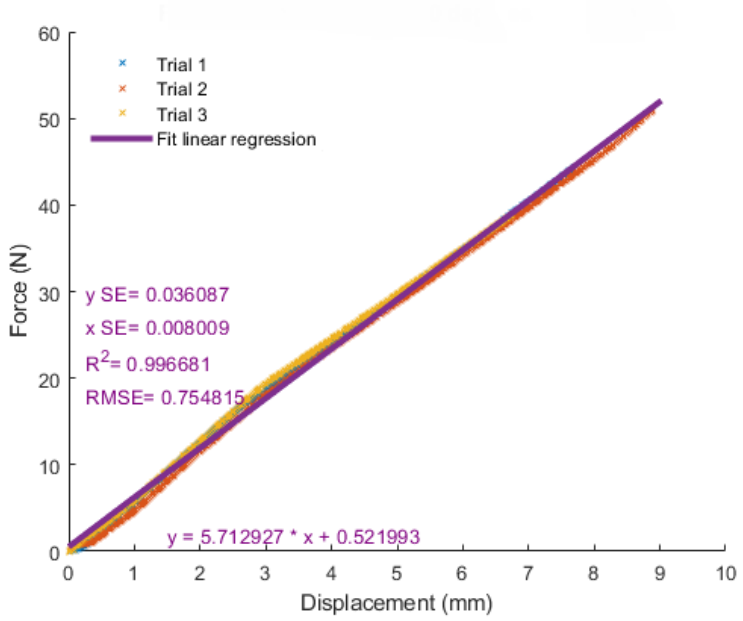

Figure 32: Experimental results of three-point bending in full extension and linear fit data.

The linear data is grouped into two zones according to the offloading profile: constant offloading, and slope to no offloading. These two zones are depicted in Figure 33. The constant offloading profile applies a constant angular displacement against the upright, whereas the slope gradually reduces the profile, reducing the displacement, until no angular displacement is applied.

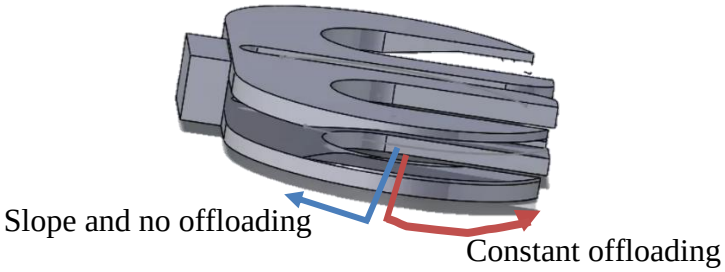

Figure 33: The two main zones of the offloading plate, in red the constant offloading profile, in blue the slope towards the no offloading.

The following graphs are visual representations of the linear fit results obtained at each angle in the two zones. Figure 34 depicts the mean linear regressions from the three trials for each angle between 0°-20°. In this range, in the constant offloading zone, the uprights are in contact with the offloading profile. The average linear slope in this section is 6.15 N/mm. This slope is larger in comparison to the second zone. As demonstrated in (4-8), the displacement is dependent on the force applied and the perpendicular length of the material. As the joint flexes, the perpendicular length decreases; thus, a larger force is required to reach the same deformation at angles 15° and 20°, compared to the closely grouped 0°-10° angles.

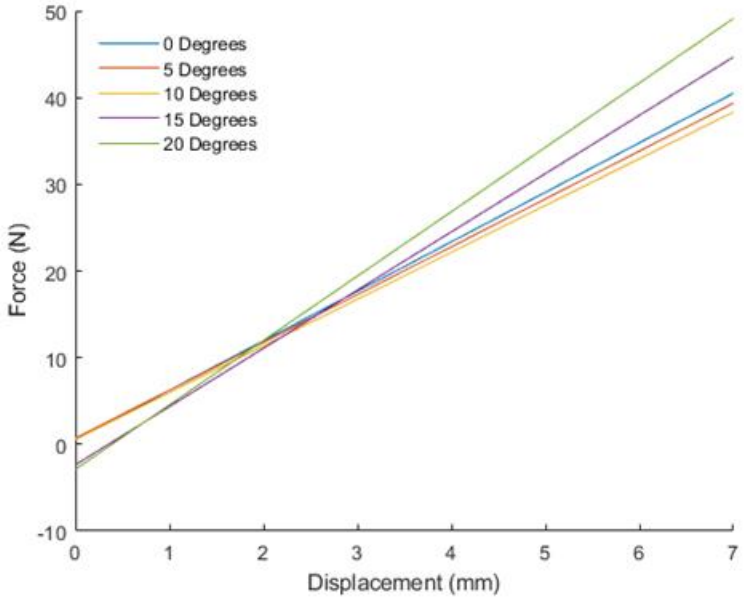

Figure 34: Summary of the linear fit results from angles 0-20 degrees. This range has angular displacement caused by the offloading profile.

The 25° and 30° data are on the slope of the offloading plate. The 35° flexion angle is on the constant no offloading profile. The average linear fits of the angles 25° to 35° are depicted in Figure 35. The 30° data has a less steep linear slope and larger RMSE than the other two angles. The variation in experimental data caused by the slipping of the upright on the slope caused a difference in slope results. As more force was applied to the joint, the uprights tended to continue down the slope at the 30° trial. This is further discussed below.

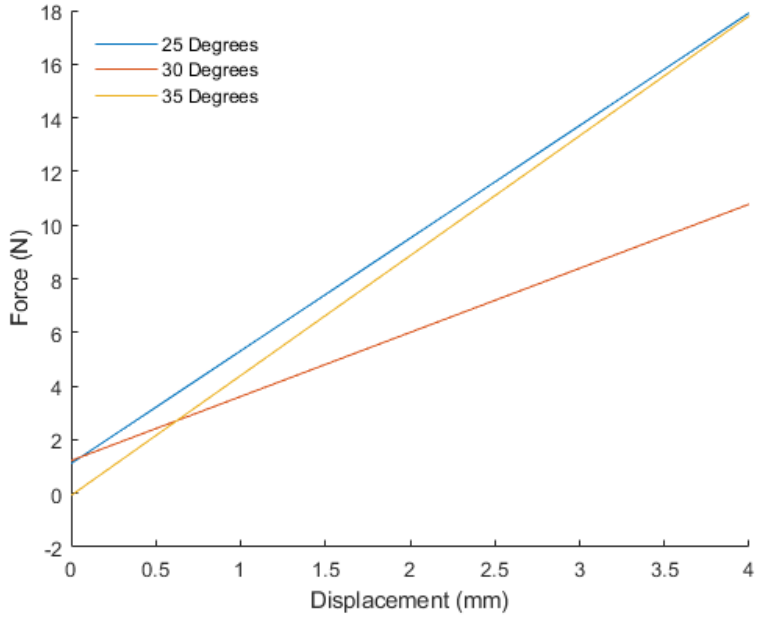

Figure 35: Summary of the linear fit results from 25 and 30 degrees. This flexion range is on the slope of the offloading profile. The 35-degree linear fit data is on the no offloading section of the joint.

In Figure 35, the displacement required to bring the brace to a neutral position is reduced compared to the first zone. Thus, the force required is also significantly lower.

Table 5 summarizes the linear fit model for each of the flexion conditions. The R^2 value remained ≥0.95 for all trials, and the RMSE was below 1.5 N for all trials.

Table 5: Summary of linear fit data for each flexion trial.

Brace Angle (°)	**Linear Fit**	**R^2**	**RMSE**
0	$y = 5.71x + 0.52$	0.997	0.75
5	$y = 5.52x + 0.71$	0.997	0.70
10	$y = 5.40x + 0.55$	0.996	0.74
15	$y = 6.72x - 2.37$	0.992	1.33
20	$y = 7.43x - 2.89$	0.99	1.49
25	$y = 4.2x + 1.11$	0.986	1.07
30	$y = 2.39x + 1.22$	0.95	1.08
35	$y = 4.47x - 0.08$	0.996	0.41

The linear fit equations presented in Table 5 will be used to calculate the force required for each angle to deflect the brace to the neutral position. The force will then be used to calculate the moment generated by the joint at each angle. The results are shown in 5.4.

5.3 Stiffness

Stiffness of the joint was listed as an essential criterion of the design. In the iterative design process, reference stiffness values from current orthoses were used as the starting point to approximate deflection.

Figure 36 demonstrates the graphical comparison of the current mediolateral stiffness of a single joint measured by force required to deflect the joint by 0.5 in (or 1.27 cm). The orthoses from left to right are as follows: Breg (unknown model) at 8.44 N/mm, Ossur Generation II OA brace at 9.32 N/mm, the DonJoy OA Defiance brace at 9.35 N/mm, the proposed joint design at 9.73 N/mm, the Townsend Premier OA brace at 13.8 N/mm, and the Ossur CTI brace at 33.69 N/mm. All braces are double upright.

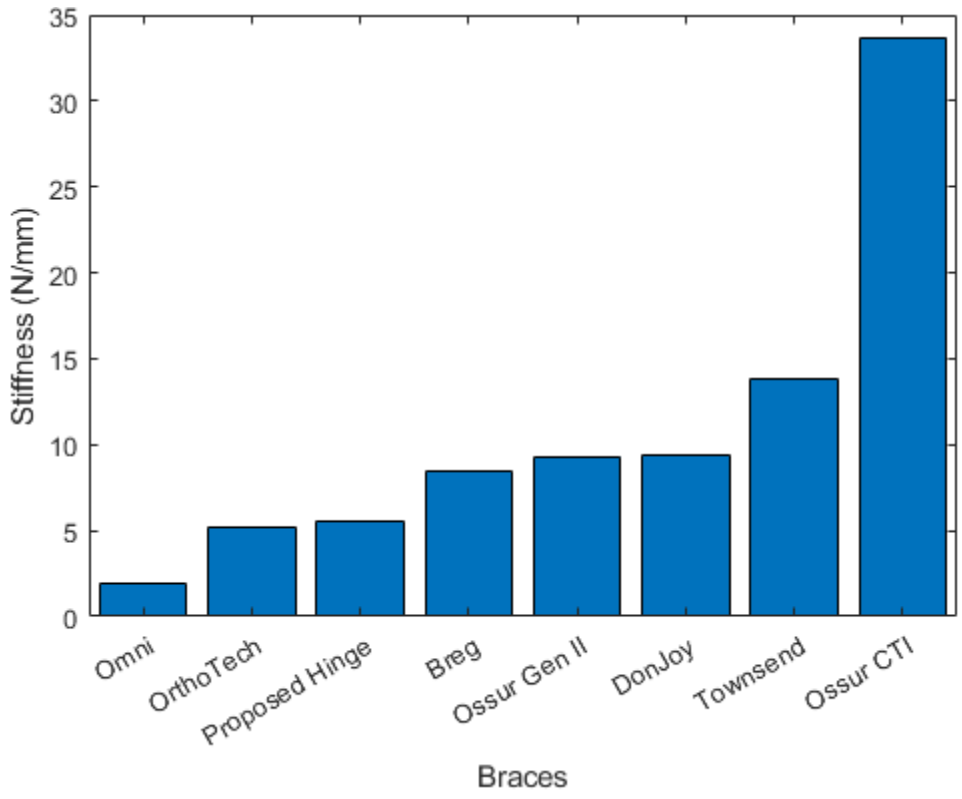

Figure 36: Comparison of brace stiffness measured by moving a single brace joint mediolaterally and normalized by millimetre. This graph includes data from [90].

The stiffness of the proposed joint is 5.58 N/mm. This is calculated using the linear fit in full extension, inserting the 1.27 cm displacement and solving for the force. As modularity and adjustability were also an identified criteria of the design, this novel variable offloading joint could be incorporated in a range of other devices with similar stiffness, such as the OrthoTech, Breg or Ossur Gen II. Also, this could be a cost-effective way to modify an existing brace with a similar stiffness to increase the comfort and perceived effect of the user.

5.4 Offloading Moment

The experimental data were graphed using interpolation between the experimental values with piecewise cubic Hermite interpolating polynomial (PCHIP), which will provide less overshoot than using a standard cubic spline or Akima interpolation. This graphing allowed for the display of the bending moment created by the offloading joint. The expected behaviour of the bending moment is expected to be piecewise and linear, not oscillatory, which makes (PCHIP) a better option. The moment was calculated using the forces required to displace the uprights to a neutral position and the perpendicular length of the uprights with respect to the flexion angle. The results are shown in Figure 37.

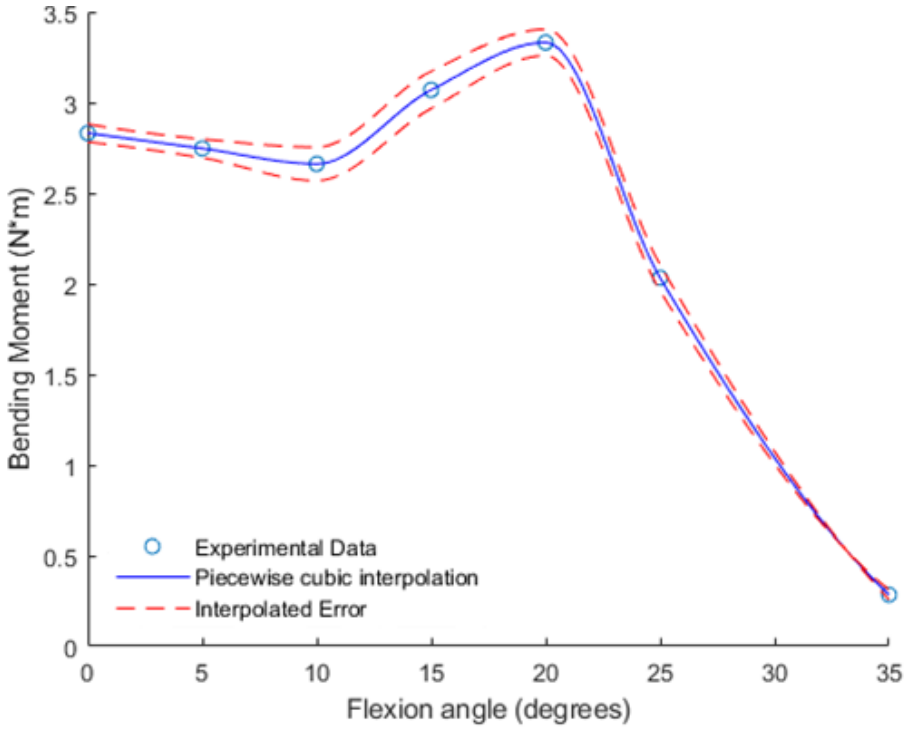

Figure 37: Offloading moment vs flexion angle.

In the offloading zone, between 0°-20°, the minimum moment is 2.56 Nm at 10°, and the maximum is 3.36 Nm. Using the average OA patient described in section 3.1 of 80 kg as the divisor, and the 10° and 20° moment, the offloading moment of the proposed joint is between 0.032 and 0.042 Nm/kg (0° to 20°). The minimum is close to the range, whereas the maximum offloading moment is within the range of 0.038 to 0.133 Nm/kg given in the literature [54], [91], [109]. This magnitude of offloading should provide a perceivable effect to the user. However, if larger magnitudes of offloading are needed, the offload plate profile can be altered to increase the available deflection to a user's leg. The joint should be tested in gait trials to determine how the offloading moment translates to reducing KAM, as the literature indicates that differences in KAM between unbraced and braced conditions can not solely be attributed to the offloading orthosis. Other elements such as changes in gait kinematics from wearing the brace may also impact the post-brace KAM moment [91].

The offloading moment decreases after 20°. At 35° flexion, a minimal moment is applied due to the contact between the offloading ramp and the upright. This reduction in applied force is expected to help increase patient comfort.

Figure 37 demonstrates the success of the proposed variable offloading design, where a greater moment is applied in 0° to 20° of flexion and decreases at the 25° to 35° measurements.

5.5 Evaluation of Comfort and Other Design Criteria

An example of pressure distribution is plotted in Figure 38. The applied force at the joint was used to plot against a sample set of surface areas. The pressure was calculated as the quotient of force and area, assuming a uniform distribution. The surface area of the knee pad and its pressure are circled in the graph. The maximum pressure tolerance greatly exceeds the limits of the y axis of the graph, thus this criterion is satisfied. The lowest pain pressure threshold found in literature is 98066.5 Pa and is greater than the proposed pressure, thus this criterion is also satisfied, it can be seen in Figure 38 [99], [102]. Therefore, it is not expected that the pressure applied by the brace or straps would cause pain. The graph demonstrates that the applied pressure at the knee pad would be above ischemic levels if it is directly applied to the knee. The straps applying the offloading force at the thigh and calf would have half the pressure; thus, the interface at the extremities would need a minimum surface area of approximately 0.0032 m^2 to be at the ischemic threshold. In case

of force transfer, the surface area at the knee would need to be enlarged to 0.0064 m^2. An example calculation is found in section 3.5.1.

The proposed offloading design does not implement direct force such as a pneumatic bladder or telescoping knee pad to apply force to the knee. This design uses the uprights to produce the bending moment; thus, the full force is not expected to be applied to the knee. However, as ischemia is a safety concern, the design would need pressure distribution testing.

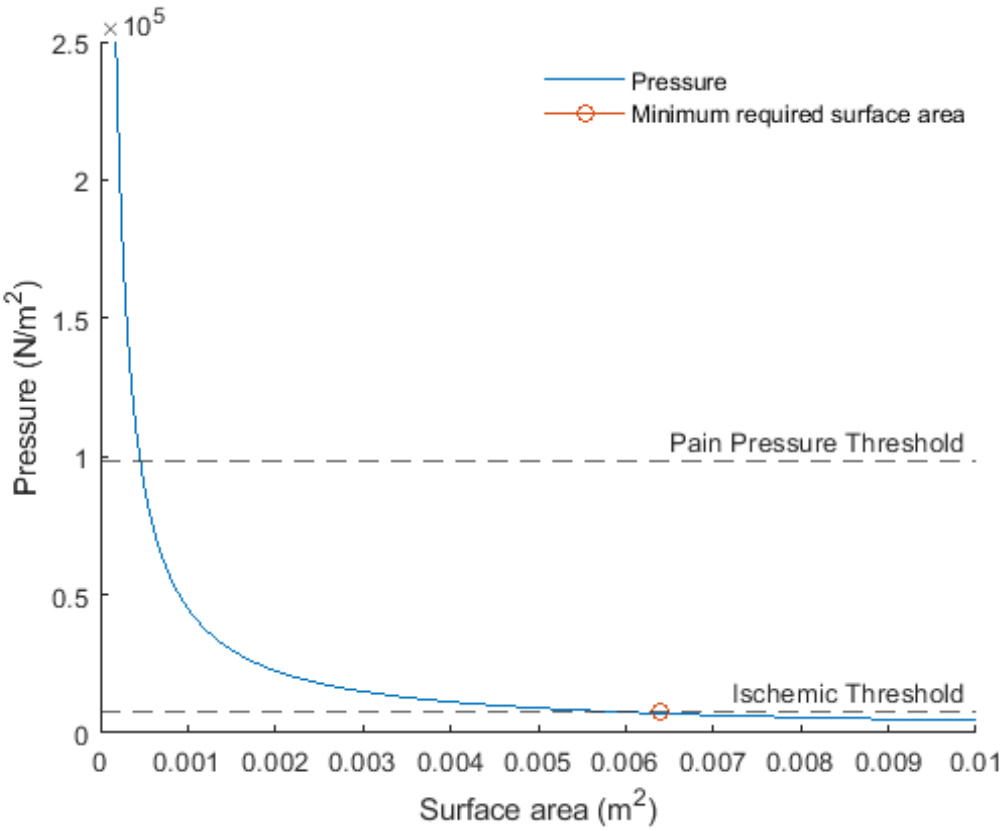

Figure 38: Pressure distribution using applied force and sample set of surface areas.

Future designs of offloading plates with higher magnitudes of offloading will need to consider the ischemic threshold, as the force required to generate a greater offloading moment will need to be increased, increasing pressure. The knee pad, calf strapping and frame will add pressure to bony prominences; thus, there is a need to consider the pain thresholds of the OA patient [99].

A recent study on exoskeleton comfort regarding pressure and padding demonstrated that the padding thickness has less effect than the distribution of the forces creating the pressure [122].

This suggests that the joint can be fitted with a thin stiff pad to better distribute the forces about the knee, increase comfort, and help keep the joint profile thin. The metal joint assembly with face covers is 1.5 cm thick, excluding the butterfly nuts. The butterfly nuts add 1 cm. The total thickness of the joint prototype falls within the maximum 3 cm recommended in Chapter 3-. It leaves an additional 0.5 cm for padding. The design weighs approximately 114 g, taking into consideration it is not a complete orthosis, and needing at least three more sections of similar length (for top, bottom, and opposite side), the orthosis would likely weigh approximately 600 g, less than the maximum of 1.25% bodyweight design criteria for the sample patient.

Braces, both off-the-shelf and custom, need to be adjusted to the patient to help increase comfort. A custom orthosis is recommended to increase comfort, although some off-the-shelf braces, such as the Medi M4 OA brace, encourage clinicians to use steel bending tools to bend the aluminum uprights to fit the patient better. This includes adjustments relative to the *q* angle of the patient, an angle measured between the patella and the anterior superior iliac spine. Alternatively, a patient could use the changeable offloading plate to adjust the uprights to fit their needs in terms of both *q* angle and offloading.

Using the existing standard of the joint uprights with gear teeth allows the brace to be compatible with flexion and extension stops commonly used in bracing and rehabilitation for individuals with OA. The prototype satisfies the ROM requirements and allows full flexion up to 130°. However, the handle for the offloading plate limits the flexion nearing 140°. This design area may need to be evaluated to ensure there is no damage to the uprights or offloading plate at extreme levels of flexion.

Chapter 6- Conclusions and Recommendations

This chapter summarizes the contributions of the work conducted, the limitations of the design and analysis, and recommendations of future work of offloading knee orthoses.

6.1 Study Contributions

It has been extensively demonstrated in literature that OA offloading orthoses are a cost-effective treatment to reduce pain, improve function and increase activity in the OA population. However, compliance rates remain low, with comfort and lack of perceived effect the main areas of concern.

The objective of this research was to design and evaluate a novel offloading orthosis joint. The proposed design is aimed to address issues related to comfort and perceived effect related to low patient compliance. To achieve this, the joint applies an offloading moment dynamically when it is most effective, in the stance phase of gait, instead of applying a constant magnitude of offloading like the majority of braces currently available. Thus, increasing the perceived effect in stance, and comfort for the user during swing and high flexion activities. The proposed design is modular, and a selection of offloading plates can be developed to customize the magnitude of offloading and apply it during different ranges of flexion. Initial findings demonstrate that the proposed design can produce the required offloading moment during the selected range of 0°-20° flexion.

This study provides an initial proof of concept and mechanical model that was validated with experimental testing results to assist in future research and future designs of other offloading plates. The results of this study can be used to investigate further dynamic offloading and alternative modular designs to current devices.

6.2 Limitations

There are several limitations that should be considered when interpreting the experimental results of this thesis.

The proposed design is a prototype used as a proof of concept for offloading plates and mechanical validation of the design. Further work would need to be done to develop a prototype acceptable for possible human testing to fully validate the proposed design. Example areas of work would be to: ensure the safety of the design to limit the possibility of injury, reduce pinch areas by fully encasing the joint, and developing a prototype to the prospective subjects, as the mechanical prototype was based on a theoretical patient.

The experimental testing closely followed previously published methods of 2-D three-point bending analysis of an offloading joint to determine the offloading moment. However, as the joint does create some degree of twisting and angular displacement, a 3-D analysis method could be considered in future studies to fully capture the movement of the joint. Additional work can also be done to determine if the additional angular motion has any impact on gait, or comfort for the user.

Friction was neglected in this study. Should there be excessive friction between the uprights and the offloading plate, this may cause discomfort for the user, or inhibit their ROM. While no difficulties in movement of the joint were noted during testing, adding Teflon could be considered and used in future iterations, in addition to including friction as a testing parameter.

Finally, additional comfort criteria, for example, noise of the joint, and esthetics were not considered in this study, and could potentially affect the compliance of wearing the brace.

6.3 Future Work

The experimental analysis of the prototype validated the offloading design mechanically. However future work is needed to fully validate the goal of the orthosis of increased comfort and perceived effect in comparison to other designs on the market. This would include modifying the design for human testing, with questionnaires to measure comfort and perceived effect in addition to mechanical analysis.

Future work on the design of the variable offloading joint includes wear and fatigue tests between the offloading plate and the uprights and testing the wear and lifetime of the gear teeth with the angular displacements introduced by the offloading plate.

Additional offloading plates to vary the magnitude of offloading and activation during specific ROM should be further investigated. Future research would need human testing to evaluate the impact of the proposed design on comfort and compliance compared to current devices.

Chapter 7- References

[1] S. C. Government of Canada, "Symptom onset, diagnosis and management of osteoarthritis," Sep. 17, 2014. https://www150.statcan.gc.ca/n1/pub/82-003-x/2014009/article/14087-eng.htm (accessed Jan. 28, 2019).

[2] B. Sharif *et al.*, "Projecting the direct cost burden of osteoarthritis in Canada using a microsimulation model," *Osteoarthritis and Cartilage*, vol. 23, no. 10, pp. 1654–1663, Oct. 2015, doi: 10.1016/j.joca.2015.05.029.

[3] S. J. Dixon, R. S. Hinman, M. W. Creaby, G. Kemp, and K. M. Crossley, "Knee joint stiffness during walking in knee osteoarthritis," *Arthritis Care & Research*, vol. 62, no. 1, pp. 38–44, 2010, doi: 10.1002/acr.20012.

[4] M. van der Esch, M. Steultjens, H. Wieringa, H. Dinant, and J. Dekker, "Structural joint changes, malalignment, and laxity in osteoarthritis of the knee," *Scandinavian Journal of Rheumatology.*, vol. 34, no. 4, pp. 298–301, Aug. 2005, doi: 10.1080/03009740510018651.

[5] D. Bhatia, T. Bejarano, and M. Novo, "Current interventions in the management of knee osteoarthritis," *Journal of Pharmacy and Bioallied Sciences*, vol. 5, no. 1, pp. 30–38, 2013, doi: 10.4103/0975-7406.106561.

[6] S.-Y. Jung *et al.*, "Comparative effectiveness of oral pharmacologic interventions for knee osteoarthritis: A network meta-analysis," *Modern Rheumatology*, vol. 28, no. 6, pp. 1021–1028, Nov. 2018, doi: 10.1080/14397595.2018.1439694.

[7] B. M. Saltzman and K. A. Campbell, "In knee osteoarthritis, pharmacological interventions, with the exception of acetaminophen, significantly improve pain; with intra-articular administration being more effective," *BMJ Evidence-Based Medicine*, vol. 20, no. 5, pp. 173–173, Oct. 2015, doi: 10.1136/ebmed-2015-110182.

[8] E. Yusuf, "Pharmacologic and Non-Pharmacologic Treatment of Osteoarthritis," *Curr Treat Options in Rheum*, vol. 2, no. 2, pp. 111–125, Jun. 2016, doi: 10.1007/s40674-016-0042-y.

[9] D. Gregori *et al.*, "Association of Pharmacological Treatments With Long-term Pain Control in Patients With Knee Osteoarthritis: A Systematic Review and Meta-analysis," *JAMA*, vol. 320, no. 24, pp. 2564–2579, 25 2018, doi: 10.1001/jama.2018.19319.

[10] "Pharmacological treatment of osteoarthritis of the hip and knee | British Columbia Medical Journal." https://www.bcmj.org/articles/pharmacological-treatment-osteoarthritis-hip-and-knee (accessed Jan. 28, 2019).

[11] "Direct Medical and Societal Cost of Opioid Use in Symptomatic Knee Osteoarthritis Patients in the United States," *ACR Meeting Abstracts*. https://acrabstracts.org/abstract/direct-medical-and-societal-cost-of-opioid-use-in-symptomatic-knee-osteoarthritis-patients-in-the-united-states/ (accessed Aug. 03, 2020).

[12] "Hip and Knee Replacements in Canada, 2017–2018: Canadian Joint Replacement Registry Annual Report," p. 53.

[13] C. Debette *et al.*, "Total knee arthroplasty of the stiff knee: three hundred and four cases," *Int Orthop*, vol. 38, no. 2, pp. 285–289, Feb. 2014, doi: 10.1007/s00264-013-2252-3.

[14] Z. Fishkin, D. Miller, C. Ritter, and I. Ziv, "Changes in human knee ligament stiffness secondary to osteoarthritis," *Journal of Orthopaedic Research*, vol. 20, no. 2, pp. 204–207, Mar. 2002, doi: 10.1016/S0736-0266(01)00087-0.

[15] Canadian Institute for Health Information, *Wait Times for Priority Procedures in Canada-Data Table*. Ottawa, ON, 2020.

[16] D. A. Mistry, A. Chandratreya, and P. Y. F. Lee, “An Update on Unloading Knee Braces in the Treatment of Unicompartmental Knee Osteoarthritis from the Last 10 Years: A Literature Review,” *Surg J (N Y)*, vol. 4, no. 3, pp. e110–e118, Jul. 2018, doi: 10.1055/s-0038-1661382.

[17] F. Rannou, S. Poiraudeau, and J. Beaudreuil, “Role of bracing in the management of knee osteoarthritis:,” *Current Opinion in Rheumatology*, vol. 22, no. 2, pp. 218–222, Mar. 2010, doi: 10.1097/BOR.0b013e32833619c4.

[18] P. Y. Lee, T. G. Winfield, S. R. Harris, E. Storey, and A. Chandratreya, “Unloading knee brace is a cost-effective method to bridge and delay surgery in unicompartmental knee arthritis,” *BMJ Open Sport and Exercise Medicine*, vol. 2, no. 1, p. e000195, 2016, doi: 10.1136/bmjsem-2016-000195.

[19] E. Squyer, D. L. Stamper, D. T. Hamilton, J. A. Sabin, and S. S. Leopold, “Unloader knee braces for osteoarthritis: do patients actually wear them?,” *Clinical Orthopaedics and Related Research*, vol. 471, no. 6, pp. 1982–1991, Jun. 2013, doi: 10.1007/s11999-013-2814-0.

[20] D. K. Ramsey and M. E. Russell, “Unloader Braces for Medial Compartment Knee Osteoarthritis: Implications on Mediating Progression,” *Sports Health*, vol. 1, no. 5, pp. 416–426, Sep. 2009, doi: 10.1177/1941738109343157.

[21] B. L. Wise *et al.*, “Patterns of Compartment Involvement in Tibiofemoral Osteoarthritis in Men and Women and in Caucasians and African Americans: the Multicenter Osteoarthritis Study,” *Arthritis Care and Research s (Hoboken)*, vol. 64, no. 6, pp. 847–852, Jun. 2012, doi: 10.1002/acr.21606.

[22] R. K. Jones *et al.*, “A New Approach to Prevention of Knee Osteoarthritis: Reducing Medial Load in the Contralateral Knee,” *The Journal of Rheumatology*, vol. 40, no. 3, pp. 309–315, Mar. 2013, doi: 10.3899/jrheum.120589.

[23] E. Losina *et al.*, “Lifetime risk and age of diagnosis of symptomatic knee osteoarthritis in the US,” *Arthritis Care and Research (Hoboken)*, vol. 65, no. 5, May 2013, doi: 10.1002/acr.21898.

[24] D. Hayashi, F. W. Roemer, and A. Guermazi, “Imaging for osteoarthritis,” *Annals of Physical and Rehabilitation Medicine*, vol. 59, no. 3, pp. 161–169, Jun. 2016, doi: 10.1016/j.rehab.2015.12.003.

[25] S. J. Newberry *et al.*, *Executive Summary*. Agency for Healthcare Research and Quality (US), 2017.

[26] A. Mündermann, C. O. Dyrby, and T. P. Andriacchi, “Secondary gait changes in patients with medial compartment knee osteoarthritis: Increased load at the ankle, knee, and hip during walking,” *Arthritis & Rheumatism*, vol. 52, no. 9, pp. 2835–2844, Sep. 2005, doi: 10.1002/art.21262.

[27] M. Henriksen, T. Graven-Nielsen, J. Aaboe, T. P. Andriacchi, and H. Bliddal, “Gait changes in patients with knee osteoarthritis are replicated by experimental knee pain,” *Arthritis Care and Research (Hoboken)*, vol. 62, no. 4, pp. 501–509, Apr. 2010, doi: 10.1002/acr.20033.

[28] J. Favre and B. M. Jolles, “Gait analysis of patients with knee osteoarthritis highlights a pathological mechanical pathway and provides a basis for therapeutic interventions,” *EFORT Open Reviews*, vol. 1, no. 10, pp. 368–374, Oct. 2016, doi: 10.1302/2058-5241.1.000051.

[29] T. Miyazaki, M. Wada, H. Kawahara, M. Sato, H. Baba, and S. Shimada, “Dynamic load at baseline can predict radiographic disease progression in medial compartment knee osteoarthritis,” *Annals of Rheumatic Diseases.*, vol. 61, no. 7, pp. 617–622, Jul. 2002.

[30] T. L. Heiden, D. G. Lloyd, and T. R. Ackland, “Knee joint kinematics, kinetics and muscle co-contraction in knee osteoarthritis patient gait,” *Clinical Biomechancic (Bristol, Avon)*, vol. 24, no. 10, pp. 833–841, Dec. 2009, doi: 10.1016/j.clinbiomech.2009.08.005.

[31] I. McCarthy, D. Hodgins, A. Mor, A. Elbaz, and G. Segal, “Analysis of knee flexion characteristics and how they alter with the onset of knee osteoarthritis: a case control study,” *BMC Musculoskeletal Disorders*, vol. 14, no. 1, p. 169, May 2013, doi: 10.1186/1471-2474-14-169.

[32] J. Favre, J. C. Erhart-Hledik, and T. P. Andriacchi, “Age-related differences in sagittal-plane knee function at heel-strike of walking are increased in osteoarthritic patients,” *Osteoarthritis and Cartilage*, vol. 22, no. 3, pp. 464–471, Mar. 2014, doi: 10.1016/j.joca.2013.12.014.

[33] A. J. Accettura, E. C. Brenneman, P. W. Stratford, and M. R. Maly, “Knee Extensor Power Relates to Mobility Performance in People With Knee Osteoarthritis: Cross-Sectional Analysis,” *Physical Therapy*, vol. 95, no. 7, pp. 989–995, Jul. 2015, doi: 10.2522/ptj.20140360.

[34] S. C. Petterson, P. Barrance, T. Buchanan, S. Binder-Macleod, and L. Snyder-Mackler, “Mechanisms Underlying Quadriceps Weakness in Knee Osteoarthritis,” *Medicine and Science in Sports and Exercise*, vol. 40, no. 3, pp. 422–427, Mar. 2008, doi: 10.1249/MSS.0b013e31815ef285.

[35] C. Slemenda *et al.*, “Quadriceps weakness and osteoarthritis of the knee,” *Annals of Internal Medicine.*, vol. 127, no. 2, pp. 97–104, Jul. 1997.

[36] S. Ikeda, H. Tsumura, and T. Torisu, “Age-related quadriceps-dominant muscle atrophy and incident radiographic knee osteoarthritis,” *Journal of Orthopaedic Science*, vol. 10, no. 2, pp. 121–126, 2005, doi: 10.1007/s00776-004-0876-2.

[37] M. V. Hurley and D. J. Newham, “The influence of arthrogenous muscle inhibition on quadriceps rehabilitation of patients with early, unilateral osteoarthritic knees,” *British Journal of Rheumatology*, vol. 32, no. 2, pp. 127–131, Feb. 1993.

[38] D. H. Spinoso, N. C. Bellei, N. R. Marques, and M. T. Navega, “Quadriceps muscle weakness influences the gait pattern in women with knee osteoarthritis,” *Advances in Rheumatology*, vol. 58, no. 1, p. 26, Aug. 2018, doi: 10.1186/s42358-018-0027-7.

[39] T. L. Heiden, D. G. Lloyd, and T. R. Ackland, “Knee extension and flexion weakness in people with knee osteoarthritis: is antagonist cocontraction a factor?,” *Journal of Orthopawedic and Sports Physical Therapy*, vol. 39, no. 11, pp. 807–815, Nov. 2009, doi: 10.2519/jospt.2009.3079.

[40] A. H. Alnahdi, J. A. Zeni, and L. Snyder-Mackler, “Muscle Impairments in Patients With Knee Osteoarthritis,” *Sports Health*, vol. 4, no. 4, pp. 284–292, Jul. 2012, doi: 10.1177/1941738112445726.

[41] T. Hortobágyi *et al.*, “Altered hamstring-quadriceps muscle balance in patients with knee osteoarthritis,” *Clinical Biomechancics (Bristol, Avon)*, vol. 20, no. 1, pp. 97–104, Jan. 2005, doi: 10.1016/j.clinbiomech.2004.08.004.

[42] A. R. Hafez *et al.*, “Treatment of Knee Osteoarthritis in Relation to Hamstring and Quadriceps Strength,” *Journal of Physical Therapy Science*, vol. 25, no. 11, pp. 1401–1405, Nov. 2013, doi: 10.1589/jpts.25.1401.

[43] M. R. Maly, P. A. Costigan, and S. J. Olney, “Contribution of psychosocial and mechanical variables to physical performance measures in knee osteoarthritis,” *Physical Therapy*, vol. 85, no. 12, pp. 1318–1328, Dec. 2005.

[44] K. R. Vincent and H. K. Vincent, “Resistance Exercise for Knee Osteoarthritis,” *Physical Medicine and Rehabilitation*, vol. 4, no. 5 0, pp. S45–S52, May 2012, doi: 10.1016/j.pmrj.2012.01.019.
[45] J. Knoop *et al.*, “Proprioception in knee osteoarthritis: a narrative review,” *Osteoarthritis and Cartilage*, vol. 19, no. 4, pp. 381–388, Apr. 2011, doi: 10.1016/j.joca.2011.01.003.
[46] Robert Topp and Pifer Matthew, “A preliminary Study Into the Effect of 2 Resistance Training Modes on Proprioception of Subjects with Knee Osteoarthritis,” *Journal of Performance Health Research*, vol. 1, no. 1, pp. 26–38, 2017, doi: 10.25036/jphr.2017.1.1.topp.
[47] S.-B. Ju, G. D. Park, and S.-S. Kim, “Effects of proprioceptive circuit exercise on knee joint pain and muscle function in patients with knee osteoarthritis,” *Journal of Physical Therapy Science*, vol. 27, no. 8, pp. 2439–2441, Aug. 2015, doi: 10.1589/jpts.27.2439.
[48] R. L. Mizner, S. C. Petterson, J. E. Stevens, M. J. Axe, and L. Snyder-Mackler, “Preoperative quadriceps strength predicts functional ability one year after total knee arthroplasty,” *Journal of Rheumatology.*, vol. 32, no. 8, pp. 1533–1539, Aug. 2005.
[49] K. J. Saleh *et al.*, “Quadriceps strength in relation to total knee arthroplasty outcomes,” *Instructional Course Lectures*, vol. 59, pp. 119–130, 2010.
[50] D. K. Ramsey and M. E. Russell, “Unloader Braces for Medial Compartment Knee Osteoarthritis,” *Sports Health*, vol. 1, no. 5, pp. 416–426, Sep. 2009, doi: 10.1177/1941738109343157.
[51] F. E. Pollo, J. C. Otis, S. I. Backus, R. F. Warren, and T. L. Wickiewicz, “Reduction of medial compartment loads with valgus bracing of the osteoarthritic knee,” *American Journal of Sports Medicine*, vol. 30, no. 3, pp. 414–421, Jun. 2002, doi: 10.1177/03635465020300031801.
[52] A. Kirkley *et al.*, “The Effect of Bracing on Varus Gonarthrosis*,” *The Journal of Bone & Joint Surgery*, vol. 81, no. 4, pp. 539–548, Apr. 1999.
[53] K. Nagai, S. Yang, F. H. Fu, and W. Anderst, “Unloader Knee Brace Increases Medial Compartment Joint Space During Gait In Knee Osteoarthritis Patients,” *Orthopaedic Journal of Sports Medicine*, vol. 6, no. 7_suppl4, p. 2325967118S0011, Jul. 2018, doi: 10.1177/2325967118S00119.
[54] W. Petersen *et al.*, “Biomechanical effect of unloader braces for medial osteoarthritis of the knee: a systematic review (CRD 42015026136),” *Archives of Orthopaedic and Trauma Surgery*, vol. 136, pp. 649–656, 2016, doi: 10.1007/s00402-015-2388-2.
[55] “Osteoarthritic Knee Braces on the Market: A Literature... : JPO: Journal of Prosthetics and Orthotics,” *LWW*. https://dev-journals2013.lww.com/jpojournal/Fulltext/2014/01000/Osteoarthritic_Knee_Braces_on_the_Market___A.2.aspx (accessed Jan. 30, 2019).
[56] Y. Dessery, É. L. Belzile, S. Turmel, and P. Corbeil, “Comparison of three knee braces in the treatment of medial knee osteoarthritis,” *The Knee*, vol. 21, no. 6, pp. 1107–1114, Dec. 2014, doi: 10.1016/j.knee.2014.07.024.
[57] J. N. Farr *et al.*, “Physical Activity Levels in Early Knee Osteoarthritis Patients Measured by Accelerometry,” *Arthritis and Rheumatology*, vol. 59, no. 9, pp. 1229–1236, Sep. 2008, doi: 10.1002/art.24007.
[58] N. S. Niazi, S. N. K. Niazi, S. B. H. Jafree, K. N. Khan, and M. Iqbal, “Role of un-loader bracing in the management of medial compartment knee osteoarthritis,” p. 4.

[59] Y. Kirane, R. Zifchock, L. Gulotta, G. Garrison, and H. Hillstrom, "554 knee pain structure and function after one year of unloader bracing for medial knee osteoarthritis," *Osteoarthritis and Cartilage*, vol. 18, pp. S248–S249, Oct. 2010, doi: 10.1016/S1063-4584(10)60581-X.
[60] T. E. Hewett, F. R. Noyes, S. D. Barber-Westin, and T. P. Heckmann, "Decrease in knee joint pain and increase in function in patients with medial compartment arthrosis: a prospective analysis of valgus bracing," *Orthopedics*, vol. 21, no. 2, pp. 131–138, Feb. 1998.
[61] M. Deie *et al.*, "The Effects of an Unloading Knee Brace and Insole with Subtalar Strapping for Medial Osteoarthritis of the Knee," *International Journal of Clinical Medicine*, vol. 04, p. 6, Dec. 2013, doi: 10.4236/ijcm.2013.412A2002.
[62] R. K. Jones *et al.*, "A comparison of the biomechanical effects of valgus knee braces and lateral wedged insoles in patients with knee osteoarthritis," *Gait & Posture*, vol. 37, no. 3, pp. 368–372, Mar. 2013, doi: 10.1016/j.gaitpost.2012.08.002.
[63] C. H. F. Pagani, M. Hinrichs, and G.-P. Brüggemann, "Kinetic and kinematic changes with the use of valgus knee brace and lateral wedge insoles in patients with medial knee osteoarthritis," *Journal of Orthopaedic Research*, vol. 30, no. 7, pp. 1125–1132, 2012, doi: 10.1002/jor.22032.
[64] M. Maleki, M. Arazpour, M. Joghtaei, S. W. Hutchins, A. Aboutorabi, and A. Pouyan, "The effect of knee orthoses on gait parameters in medial knee compartment osteoarthritis: A literature review," *Prosthetics and Orthotics International*, vol. 40, no. 2, pp. 193–201, Apr. 2016, doi: 10.1177/0309364614547411.
[65] M. Toriyama *et al.*, "Effects of unloading bracing on knee and hip joints for patients with medial compartment knee osteoarthritis," *Clinical Biomechanics*, vol. 26, no. 5, pp. 497–503, Jun. 2011, doi: 10.1016/j.clinbiomech.2011.01.003.
[66] S. Phillips *et al.*, "Treatment of Osteoarthritis of the Knee with Bracing: A Scoping Review," *Orthop Rev (Pavia)*, vol. 8, no. 2, Jun. 2016, doi: 10.4081/or.2016.6256.
[67] "OA Unloader Knee Braces - Okanagan Pedorthics and Sports Bracing," *Okaped Pedorthists Clinic Kelowna*. https://www.okaped.com/product/unloader-knee-brace/ (accessed Aug. 08, 2020).
[68] "OA Adjuster 3 | DJO Global." https://www.djoglobal.com/products/donjoy/oa-adjuster-3 (accessed Aug. 08, 2020).
[69] D. Laroche, C. Morisset, C. Fortunet, V. Gremeaux, J.-F. Maillefert, and P. Ornetti, "Biomechanical effectiveness of a distraction–rotation knee brace in medial knee osteoarthritis: Preliminary results," *The Knee*, vol. 21, no. 3, pp. 710–716, Jun. 2014, doi: 10.1016/j.knee.2014.02.015.
[70] P. Ornetti *et al.*, "Clinical effectiveness and safety of a distraction-rotation knee brace for medial knee osteoarthritis," *Annals of Physical and Rehabilitation Medicine*, vol. 58, no. 3, pp. 126–131, Jun. 2015, doi: 10.1016/j.rehab.2015.03.004.
[71] A. Diaz *et al.*, "OP0057 Efficacy and safety of a distraction-rotation knee brace (ODRA) in medial knee osteoarthritis – a phase iii randomised controlled trial (ergonomie study)," *Annals of the Rheumatic Diseases*, vol. 77, no. Suppl 2, pp. 79–79, Jun. 2018, doi: 10.1136/annrheumdis-2018-eular.4927.
[72] "OdrA orthosis : relieves the pain due to osteoarthritis." http://www.proteor.com/report,823-orthese-odra-soulager-la-douleur-de-l-arthrose-du-genou.php (accessed Aug. 08, 2020).

[73] "Knee orthosis - OdrA - Proteor - knee distraction (osteoarthritis) / open knee / articulated." https://www.medicalexpo.com/prod/proteor/product-74986-670184.html (accessed Aug. 08, 2020).
[74] J. Whiteside, "Self-aligning adjustable orthopedic joint brace," US6387066B1, May 14, 2002.
[75] "Townsend Bracing." https://www.thuasneusa.com/wp-content/uploads/2017/05/2016-Bracing-Technology_Web.pdf (accessed May 30, 2019).
[76] "DUO Knee Brace," *Breg, Inc.* https://www.breg.com/products/knee-bracing/functional-oa/duo-knee-brace/ (accessed Aug. 08, 2020).
[77] B. O. Bledsoe, "United States Patent: 9615955 - Orthopedic knee brace with dynamically changing medial and lateral hinges," 9615955, Apr. 11, 2017.
[78] J. J. Cherian, A. Bhave, B. H. Kapadia, R. Starr, M. J. McElroy, and M. A. Mont, "Strength and Functional Improvement Using Pneumatic Brace with Extension Assist for End-Stage Knee Osteoarthritis: A Prospective, Randomized trial," *The Journal of Arthroplasty*, vol. 30, no. 5, pp. 747–753, May 2015, doi: 10.1016/j.arth.2014.11.036.
[79] A. J. Johnson, R. Starr, B. H. Kapadia, A. Bhave, and M. A. Mont, "Gait and clinical improvements with a novel knee brace for knee OA," *Journal of Knee Surgery*, vol. 26, no. 3, pp. 173–178, Jun. 2013, doi: 10.1055/s-0032-1327452.
[80] B. Kapadia *et al.*, "Gait Using Pneumatic Brace for End-Stage Knee Osteoarthritis," *Journal of Knee Surgery*, vol. 29, no. 03, pp. 218–223, Mar. 2016, doi: 10.1055/s-0036-1579790.
[81] "Ortho Pro OA Rehabilitator Knee Brace - OCSI Ongoing Care Knee Brace," *www.phc-online.com*. https://www.phc-online.com/product_p/orthopro-oa.htm (accessed Oct. 22, 2018).
[82] R. A. Nace and CR, "United States Patent: 7608051 - Osteoarthritis knee orthosis," 7608051, Oct. 27, 2009.
[83] "Levitation Offloader Add-On," *Spring Loaded Technology*. https://springloadedtechnology.com/product/levitation-offloader/ (accessed Jan. 30, 2019).
[84] "Study links Spring Loaded Technology's Levitation Knee Brace to significant reduction in muscle fatigue |." http://www.orthospinenews.com/2016/09/21/study-links-spring-loaded-technologys-levitation-knee-brace-to-significant-reduction-in-muscle-fatigue/ (accessed Jan. 30, 2019).
[85] "Levitation Knee Brace," *Spring Loaded Technology*. https://springloadedtechnology.com/product/levitation-knee-brace/ (accessed Aug. 08, 2020).
[86] Garrish, Robert, "CA 2998197 Hinge for a brace," Jun. 15, 2015.
[87] K. D. Gross and H. J. Hillstrom, "Noninvasive Devices Targeting the Mechanics of Osteoarthritis," *Rheumatic Disease Clinics of North America*, vol. 34, no. 3, pp. 755–776, Aug. 2008, doi: 10.1016/j.rdc.2008.06.001.
[88] N. D. Reeves and F. L. Bowling, "Conservative biomechanical strategies for knee osteoarthritis," *Nature Reviews Rheumatology*, 2011, doi: 10.1038/nrrheum.2010.212.
[89] Robert C Juvinall and Kurt M. Marshek, "Fundamentals of Machine Component Design," 5th Ed., John Wiley & Sons, 2012, pp. 204–205.
[90] S. Sterling, "Anatomically designed orthopedic knee brace," US6969364B2, Nov. 29, 2005.

[91] B. P. Self, R. M. Greenwald, and D. S. Pflaste, “A biomechanical analysis of a medial unloading brace for osteoarthritis in the knee,” *Arthritis Care & Research*, vol. 13, no. 4, pp. 191–197, 2000, doi: 10.1002/1529-0131(200008)13:4<191::AID-ANR3>3.0.CO;2-C.
[92] R. T. Lewinson, J. T. Worobets, and D. J. Stefanyshyn, “Calculation of external knee adduction moments: A comparison of an inverse dynamics approach and a simplified lever-arm approach,” *The Knee*, vol. 22, no. 4, pp. 292–297, Sep. 2015, doi: 10.1016/j.knee.2015.04.003.
[93] D. J. Rutherford and M. Baker, “Knee moment outcomes using inverse dynamics and the cross product function in moderate knee osteoarthritis gait: A comparison study,” *Journal of Biomechanics*, vol. 78, pp. 150–154, Sep. 2018, doi: 10.1016/j.jbiomech.2018.07.021.
[94] S. Farrokhi, C. A. Voycheck, S. Tashman, and G. K. Fitzgerald, “A Biomechanical Perspective on Physical Therapy Management of Knee Osteoarthritis,” *Journal of Orthopaedic and Sports Physical Therapy*, vol. 43, no. 9, pp. 600–619, Sep. 2013, doi: 10.2519/jospt.2013.4121.
[95] Y. Nie, H. Wang, B. Xu, Z. Zhou, B. Shen, and F. Pei, “The Relationship between Knee Adduction Moment and Knee Osteoarthritis Symptoms according to Static Alignment and Pelvic Drop,” *BioMed Research International*, Dec. 27, 2019. https://www.hindawi.com/journals/bmri/2019/7603249/ (accessed Aug. 09, 2020).
[96] R. Featherstone, “Inverse Dynamics,” in *Rigid Body Dynamics Algorithms*, R. Featherstone, Ed. Boston, MA: Springer US, 2008, pp. 89–100.
[97] R. Van Hulle, C. Schwartz, V. Denoël, J.-L. Croisier, B. Forthomme, and O. Brüls, “A foot/ground contact model for biomechanical inverse dynamics analysis,” *Journal of Biomechanics*, vol. 100, p. 109412, Feb. 2020, doi: 10.1016/j.jbiomech.2019.109412.
[98] A. J. Veale and S. Q. Xie, “Towards compliant and wearable robotic orthoses: A review of current and emerging actuator technologies,” *Medical Engineering & Physics*, vol. 38, no. 4, pp. 317–325, Apr. 2016, doi: 10.1016/j.medengphy.2016.01.010.
[99] José L. Pons, *Wearable Robots: Biomechatronic Exoskeletons*. John Wiley & Sons Ltd, 2008.
[100] R. S. Goonetilleke and T. J. Eng, “Contact Area Effects on Discomfort,” *Proceedings of the Human Factors and Ergonomics Society Annual Meeting*, vol. 38, no. 10, pp. 688–690, Oct. 1994, doi: 10.1177/154193129403801032.
[101] M. Mikkelsson, P. Latikka, H. Kautiainen, R. Isomeri, and H. Isomtiki, “Muscle and Bone Pressure Pain Threshold and Pain Tolerance in Fibromyalgia Patients and Controls,” p. 5, 1992.
[102] “Talk: Pressure Pain Threshold and Knee Pain in Osteoarthritis: The Multicenter Osteoarthritis Study (2011 ACR/ARHP Annual Scientific Meeting).” https://acr.confex.com/acr/2011/webprogram/Paper19872.html (accessed May 31, 2019).
[103] V. Sharma, B. Cunniffe, A. P. Verma, M. Cardinale, and D. Yellon, “Characterization of acute ischemia-related physiological responses associated with remote ischemic preconditioning: a randomized controlled, crossover human study,” *Physiological Reports*, vol. 2, no. 11, Nov. 2014, doi: 10.14814/phy2.12200.
[104] Robert C Juvinall and Kurt M. Marshek, “Fundamentals of Machine Component Design,” 5th Ed., John Wiley & Sons, 2012, p. 63.
[105] M. Arazpour, M. A. Bani, M. Maleki, F. T. Ghomshe, R. V. Kashani, and S. W. Hutchins, “Comparison of the efficacy of laterally wedged insoles and bespoke unloader knee orthoses

in treating medial compartment knee osteoarthritis," *Prosthetics and Orthotics International*, vol. 37, no. 1, pp. 50–57, Feb. 2013, doi: 10.1177/0309364612447094.
[106] M. Brown, "A novel method to analyze the mechanics of unloader braces for medial knee osteoarthritis," 2014.
[107] "Knee Braces: Current Evidence and Clinical Recommendations for Their Use - American Family Physician." https://www.aafp.org/afp/2000/0115/p411.html (accessed Mar. 21, 2019).
[108] A. J. Veale and S. Q. Xie, "Towards compliant and wearable robotic orthoses: A review of current and emerging actuator technologies," *Medical Engineering & Physics*, vol. 38, no. 4, pp. 317–325, Apr. 2016, doi: 10.1016/j.medengphy.2016.01.010.
[109] T. Schmalz, E. Knopf, H. Drewitz, and S. Blumentritt, "Analysis of biomechanical effectiveness of valgus-inducing knee brace for osteoarthritis of knee," *The Journal of Rehabilitation Research and Development*, vol. 47, no. 5, p. 419, 2010, doi: 10.1682/JRRD.2009.05.0067.
[110] Carolyn Jarvis, *Physical Examination and Health Assessment - Canadian - 3rd Edition*, 3rd Edition. Saunders Canada, 2018.
[111] Mirza Biscevic, Mujo Hebibovic, Dragica Smrke, "Variations of Femoral Condyle Shape," *Collegium Anthropologicum* vol. 29, no. 2, pp. 409–414, Apr. 2005.
[112] S. M. Howell, S. J. Howell, and M. L. Hull, "Assessment of the Radii of the Medial and Lateral Femoral Condyles in Varus and Valgus Knees with Osteoarthritis:," *The Journal of Bone and Joint Surgery-American Volume*, vol. 92, no. 1, pp. 98–104, Jan. 2010, doi: 10.2106/JBJS.H.01566.
[113] Eckhoff, Donald, Hogan, Craig, DiMatteo, Laura, Robinson, Mitch, and Bach, Joel, "Difference Between the Epicondylar and Cylindrical Axis of the Knee," *Clinical Orthopaedics and Related Research*, vol. 461, pp. 238–244.
[114] "National Health Statistics Reports, Number 122, December 20, 2018," no. 122, p. 16, 2018.
[115] "Fusion® OA Plus Osteoarthritis Knee Brace," *Breg, Inc.* https://www.breg.com/products/knee-bracing/functional-oa/fusion-oa-knee-brace/ (accessed Feb. 07, 2021).
[116] Ossur, "Ossur Catalog." 2019, Accessed: Feb. 07, 2021. [Online]. Available: https://assets.ossur.com/library/41010.
[117] "ASM Material Data Sheet." http://asm.matweb.com/search/SpecificMaterial.asp?bassnum=MA6061T6 (accessed Jul. 29, 2020).
[118] "GE 5 E | SKF." https://www.skf.com/ca/en/products/plain-bearings/spherical-plain-bearings-rod-ends/radial/productid-GE%205%20E (accessed Feb. 15, 2021).
[119] Richard T. Barrett, "Fastner Design Manual," in *NASA Reference publication 1228*, NASA, 1990, p. 20.
[120] Robert C Juvinall and Kurt M. Marshek, "Fundamentals of Machine Component Design," 5th Ed., John Wiley & Sons, 2012, pp. 207–208.
[121] Robert C Juvinall and Kurt M. Marshek, "Fundamentals of Machine Component Design," 5th Ed., John Wiley & Sons, 2012, p. Appendix B-1a.
[122] L. Levesque, S. Pardoel, Z. Lovrenovic, and M. Doumit, "Experimental comfort assessment of an active exoskeleton interface," in *2017 IEEE International Symposium on Robotics and Intelligent Sensors (IRIS)*, Oct. 2017, pp. 38–43, doi: 10.1109/IRIS.2017.8250095.

Appendix A. Raw Graph Data with Individual Linear Fit

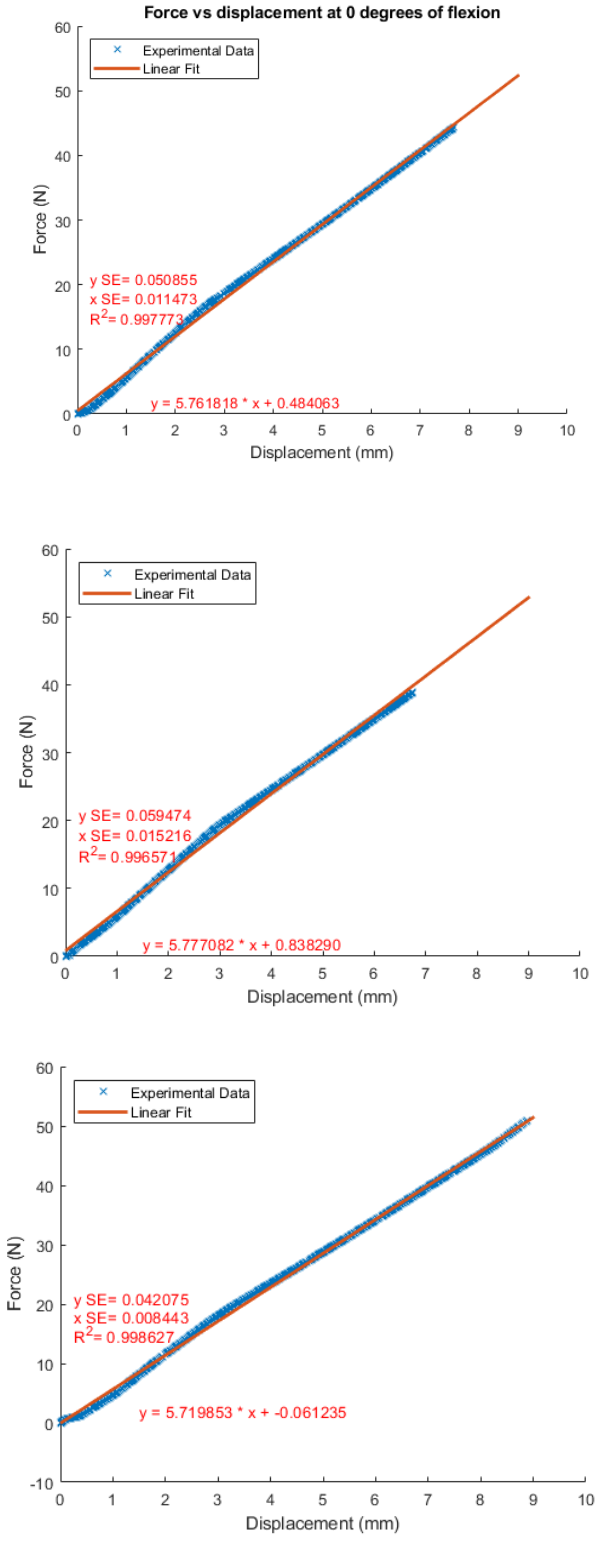

Figure 39: Experimental data, three trials at 0 degrees flexion

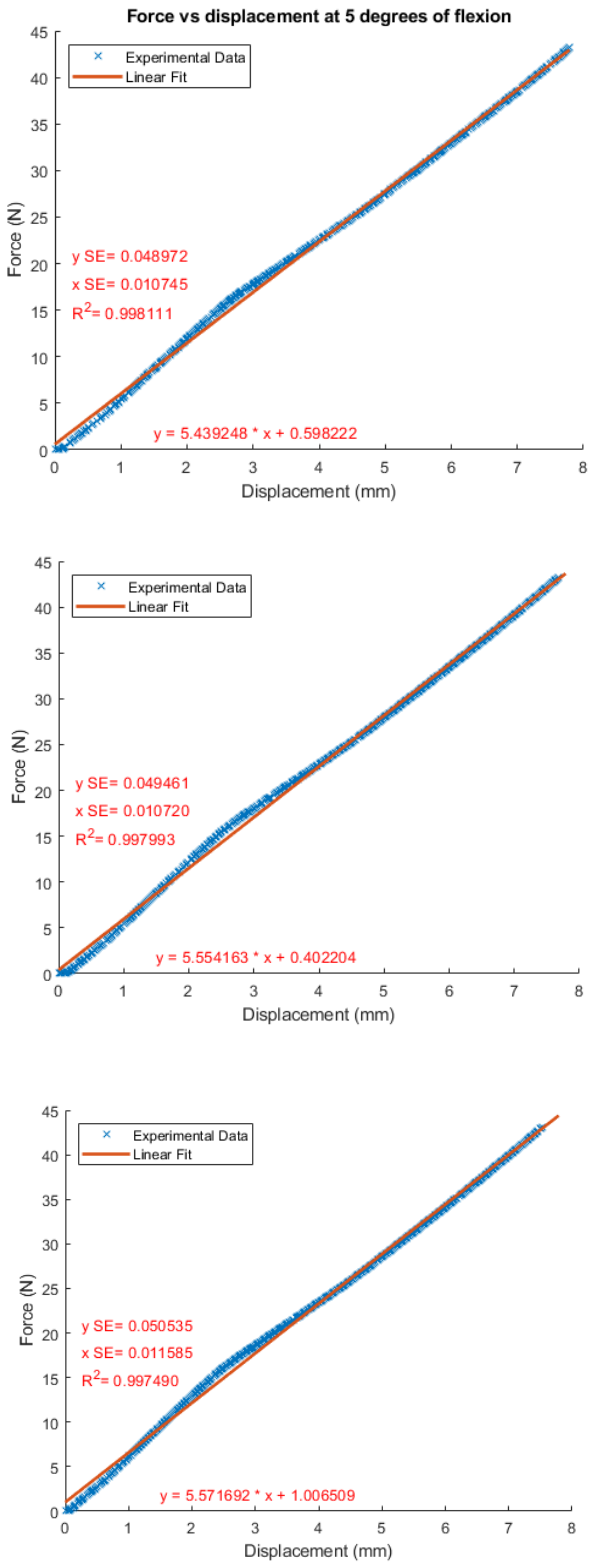

Figure 40:Experimental data, three trials at 5 degrees flexion

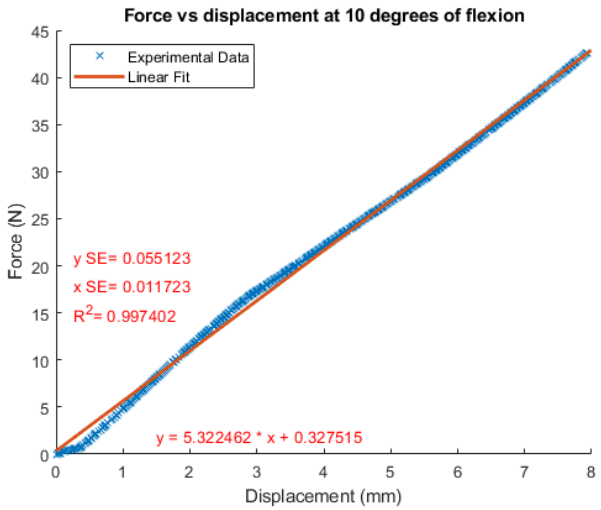

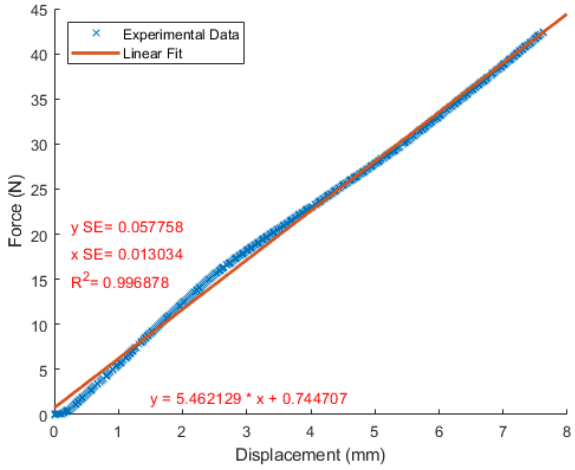

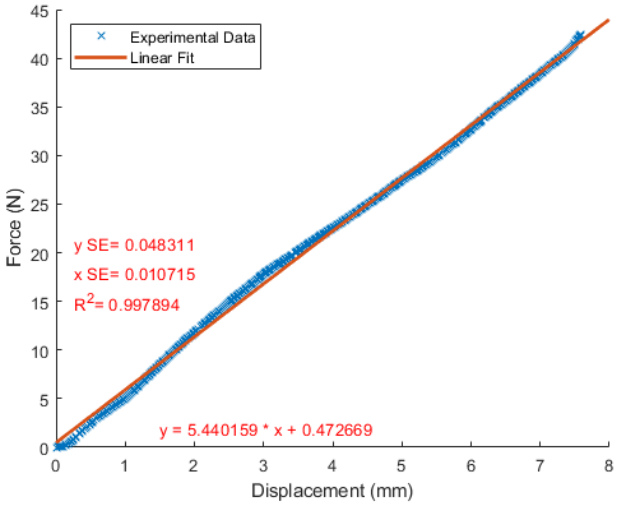

Figure 41: Experimental data, three trials at 10 degrees flexion

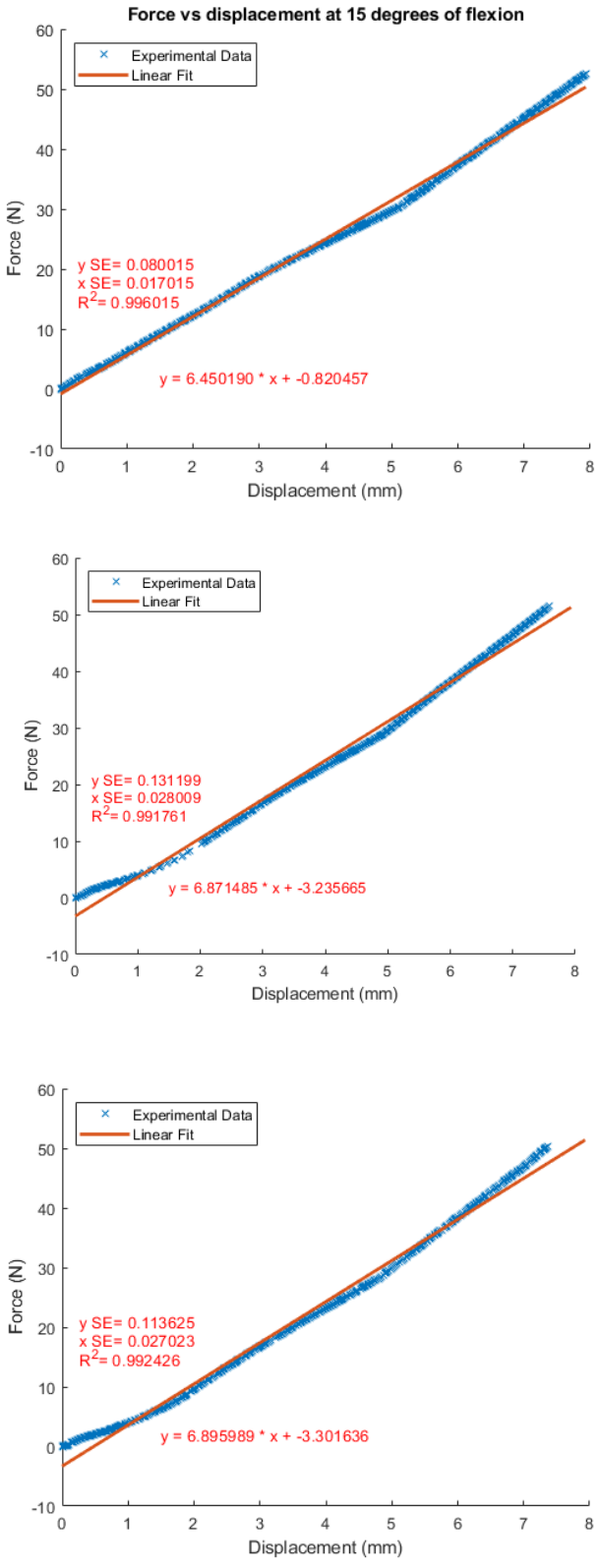

Figure 42: Experimental data, three trials at 15 degrees flexion

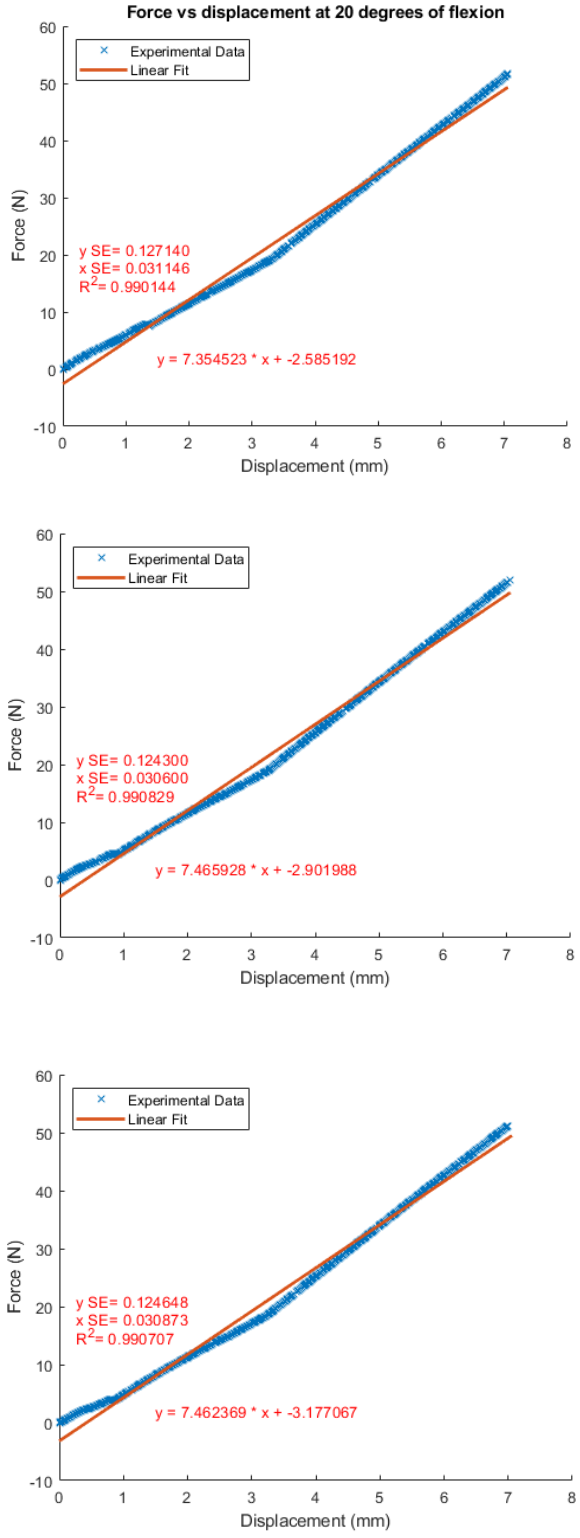

Figure 43:Experimental data, three trials at 20 degrees flexion

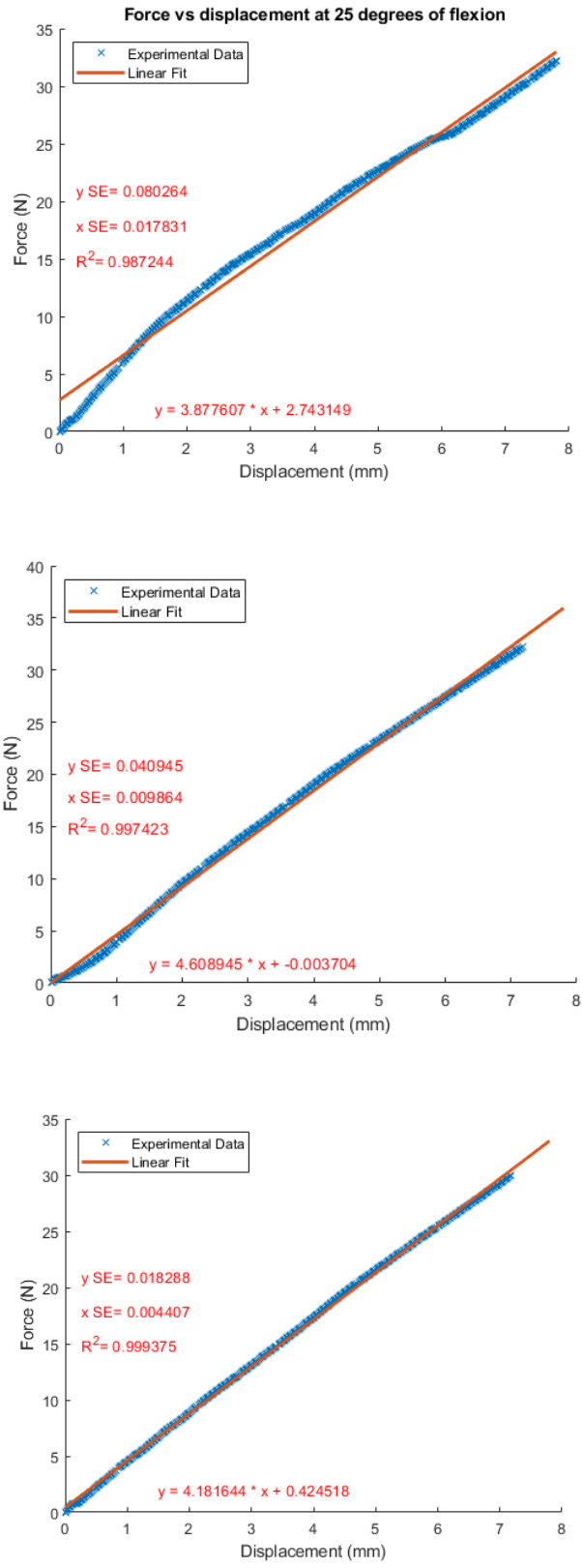

Figure 44:Experimental data, three trials at 25 degrees flexion

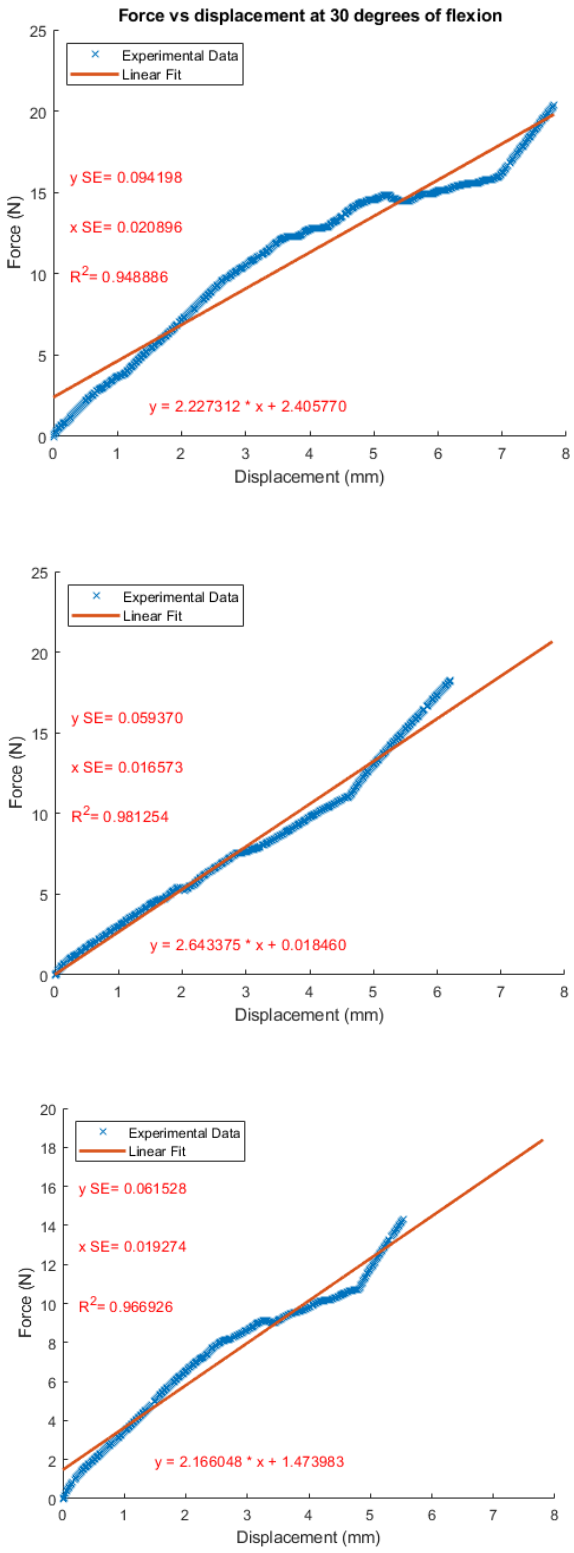

Figure 45:Experimental data, three trials at 30 degrees flexion

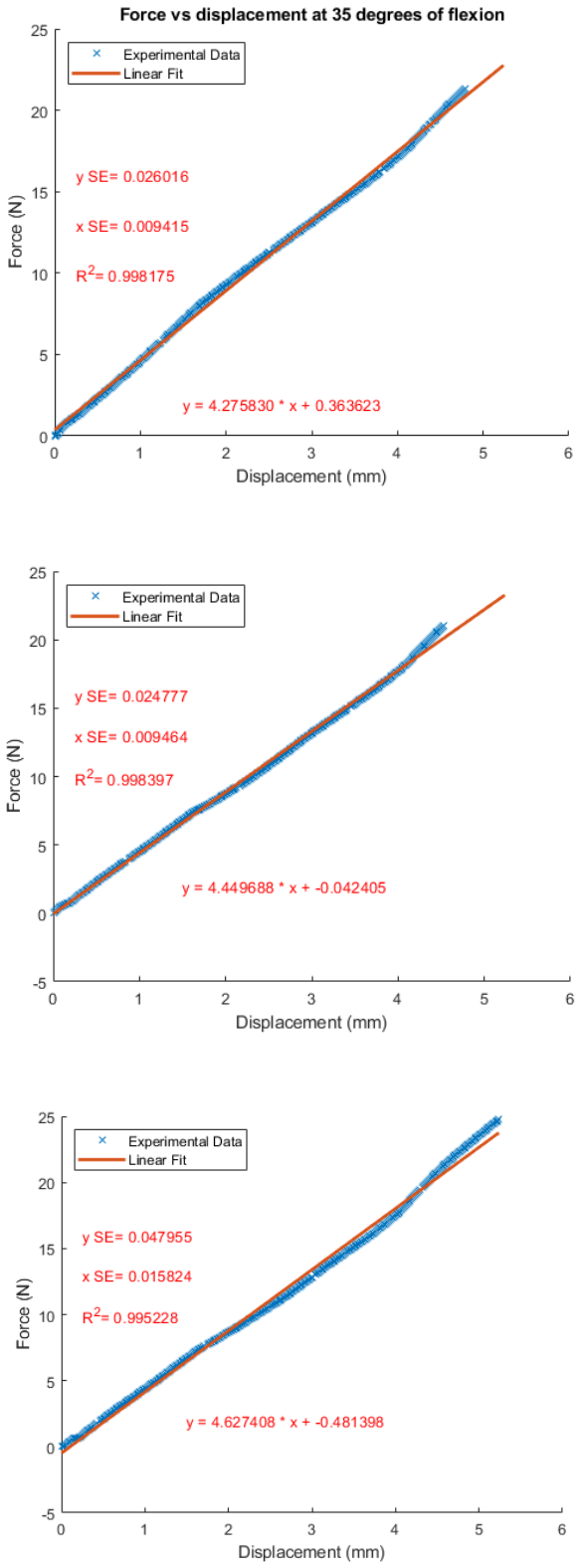

Figure 46:Experimental data, three trials at 35 degrees flexion